A LIFE-CYCLE ASSESSMENT OF CANADIAN-PRODUCED LIQUEFIED NATURAL GAS FOR CONSUMPTION IN CHINA

A REPORT SUBMITTED TO THE DEPARTMENT OF ENERGY RESOURCES ENGINEERING

OF STANFORD UNIVERSITY

IN PARTIAL FULFILLMENT OF THE REQUIREMENTS FOR THE DEGREE OF MASTER OF SCIENCE

Daniel Javier Roda-Stuart
June 2018

I certify that I have read this report and that in my opinion it is fully adequate, in scope and in quality, as partial fulfillment of the degree of Master of Science in Energy Resources Engineering.

Prof. Adam Brandt
(Principal Advisor)

Abstract

Natural gas consumption has increased in recent decades due to low prices and emissions benefits over coal. The greenhouse gas (GHG) benefits of natural gas over coal require a low upstream emissions profile, in particular with low fugitive emissions of methane. Furthermore, natural gas is unlike oil in that it is highly transport-constrained. Liquefied natural gas (LNG) allows for overseas shipping but comes at significant economic and energetic costs. We worked with a Canadian liquids-rich gas producer to better understand upstream fugitive emissions and assess their efficacy of leak detection and repair (LDAR) programs. We model emissions from their operations and perform life-cycle assessment (LCA) of a hypothetical scenario where they produce 1 billion cubic feet per day of LNG in coastal British Columbia, for consumption in Shenzhen, China. We determine the life-cycle GHG and criteria air pollutant emissions associated with such a project.

We find that the LDAR surveys have resulted in decreased number of emissions points and decreased site-wide emissions. Leaks that were fixed from LDAR surveys tended to remain fixed and did not reappear. Likewise, leaks that were not fixed tended to persist and did not go away on their own, indicating that leak persistence is very high. Consequently, LDAR surveys are resulting in emissions reductions, as long as detected leaks are fixed. Repeat LDAR surveys regularly found new emission sources, even without significant site changes occurring, supporting the idea that LDAR surveys must be done regularly to find and fix new emission sources that arise from equipment failure or breakdown.

We find that Canada-to-China LNG will result in fewer life-cycle GHG emissions than the same power generated using coal in Asian markets. Studies have estimated Chinese coal power emissions to be anywhere from 868 to 975 g CO_2e/kWh, nearly double our results of 408.2 to 547.9 g CO_2e/kWh. Our results are lower than prior studies due to low upstream emissions and more efficient LNG production assumptions. LCA studies of LNG have focused on upstream and liquefaction stages, but our work makes it clear that total emissions are dominated by end-use emissions. When considering the climate benefits and drawbacks of LNG, it is critical to understand how the gas will be used.

Acknowledgments

Thank you to Seven Generations Energy Ltd. for providing funding for this work. At 7G I would specifically like to thank Dan Stauft, Carolyn Pfau, Patrick Arnell, Tim Stauft, and Ken Woloschuk for their support and dedication to building an oil and gas company that cares about its environmental impact. Thank you, as well, to all other teams and project staff that worked on this project with me.

Thank you to my mother who has taught me to never be content with the bare minimum, my father for showing me how to prioritize what is truly important in life, and my sister for always reminding me to pursue my passions. In some ways, this thesis is a reflection of all you've taught me!

Thank you to the many ERE staff who have put up with me and helped me along the way. Specifically, Joanna Sun, Arlene Abucay, Stephanie James, and Thuy Nguyen. You all managed to always bring a smile to my face in the sometimes-overwhelming hallways of Green.

Thank you to Brad Ritts and the Stanford Natural Gas Initiative for giving me a platform to present my work, and for showing me that people are interested in the work I do.

Thank you to Jacob Englander, who took me under his wing when I was a lost freshman. You've been a great friend throughout my time at Stanford. Thank you to Dr. Arvind Ravikumar for being supportive throughout this entire project, and for always providing much-needed comic relief. I'll remember our many trips to Canada for years to come.

And lastly, thank you to the fearless leader of the Environmental Assessment and Optimization group, Dr. Adam Brandt. My five years at Stanford have been truly incredible, and you've been a big reason for that. Thank you for teaching me how to do real research, for being an understanding and supportive advisor, and for the many laughs along the way. Thank you!

Contents

List of Tables

List of Figures

Chapter 1

1 Introduction

Global demand for natural gas is growing as the drawbacks of coal loom ever larger [1]. A large-scale shift to gas is beginning in China, India, and other Asian countries, where significant health impacts are caused by poor air quality in rapidly-expanding industrial and urban centers [2]. In addition to local air and health impacts, natural gas has only half the climate-warming greenhouse gas (GHG) emissions of coal. Lastly, natural gas can be used flexibly in many applications including ramp-ready power generation for renewable support and backup. For all of these reasons, many studies of the future of global energy supply expect gas demand to grow for decades.

As demand grows, the United States (U.S.) and Canada have recently seen a dramatic increase in natural gas supply due to advances in horizontal drilling and hydraulic fracturing techniques applied to so-called “tight” or “shale” formations. For example, shale gas production in the U.S. has increased significantly: production increased from 1.3 trillion cubic feet (tcf) in 2007 to 17 tcf in 2016 [3].

This abundance has led to low natural gas prices [4]. In many shale plays, gas is a secondary, low-value product compared to crude oil or hydrocarbon (HC) liquids produced alongside it. In response, producers in Canada and the U.S. have begun to explore global markets for export. Especially since some of this gas is currently wasted via flaring, putting it to productive use has the potential to significantly reduce emissions per unit of useful energy provided.

Liquefied natural gas (LNG) is the most viable pathway to monetizing North American gas. To make LNG, natural gas is cooled to -162 °C, turning it into a liquid that allows for transportation in dense form via ship. Overseas shipping of LNG transforms gas from a regional resource constrained by pipelines to a global resource limited only by global demand and supply scenarios. While coal-to-gas switching in power generation will clearly

improve local air quality, LNG pathways are not without impacts: the process of extraction, transportation, and liquefaction of natural gas is energy-intensive.

This study takes a life-cycle approach to assessing emissions impacts associated with a proposed LNG pathway. This pathway includes Northern Canadian natural gas transported as LNG to China for either power generation or district heating. In particular, we focus on the operations of a liquids-rich natural gas producer in Northern Alberta, Canada. We model hypothetical operations for a project producing 1 billion cubic feet per day (bcf/d) of natural gas converted to LNG and shipped to Shenzhen, China for use in either power generation or district heating.

To better understand the life-cycle impacts of such a project, Seven Generations Energy Ltd. (henceforth 7G), commissioned a comparative life-cycle assessment (LCA) to be performed by three Universities: Stanford University, University of Calgary and University of British Columbia. Each university developed independent LCAs, using a diversity of methods to analyze cases with similar underlying assumptions. To maintain independence, initial collaboration between the universities was restricted to broad study assumptions with no collaboration regarding detailed process modeling. After initial results were constructed, a process of cross-comparison, peer review, and modification was performed with the teams to ensure that best practices were utilized across studies.

Stanford University took a bottom-up approach to modeling 7G's current operations. We used the Oil Production Greenhouse Gas Emissions Estimator (OPGEE) model, an open-source oil and gas GHG assessment tool developed at Stanford University. OPGEE estimates the life-cycle GHG emissions associated with the production, processing, and transmission of oil and gas products. Detailed documentation and OPGEE model files are available for free download [5]. OPGEE was supplemented with custom calculations to model 7G operations more accurately, including fugitive emissions data derived from field measurement campaigns and detailed information on plant operating data and equipment types. Some process stages, such as natural gas liquefaction, are not represented in default OPGEE modules and so were modeled using information from the literature.

Additionally, 7G allowed access to detailed data from three years of leak detection and repair (LDAR) surveys completed at their upstream facilities by contractors. These data were useful in estimating fugitive and venting emissions from 7G operations. This LDAR analysis also stands on its own, providing some of the first presented work on the effectiveness of LDAR programs and the persistence of leaks and vents over time.

In this thesis, we first discuss prior work on fugitive methane emissions and LDAR programs, as well as LCAs of upstream oil and gas production and LNG, allowing comparisons to our results. The methods and tools used in both LDAR analysis and LCA analysis are then be discussed. Next, we will present our results. Results of the LDAR work are split into emissions profiles and persistence analysis. The results of the LCA work are aggregated into five main stages: Upstream, Midstream, Liquefaction, Transport, and Downstream. Finally, we discuss major takeaways and potential future improvements to this analysis. The final operational model and calculation sheet for the LCA is available publicly through Stanford's Environmental Assessment and Optimization group website [6].

1.1 Literature Review

1.1.1 Fugitive Emissions and Leak Detection and Repair Programs

Within the past decade a number of studies have been published on fugitive methane emissions resulting from oil and gas production. One common result is that bottom-up and top-down estimates often do not align when the same region is studied using measurements at different scales [7]. Another key insight is that the majority of emissions come from so-called "super-emitters" [8], such that the largest 5% of emissions sources contribute over 50% of the leakage volume. It is also clear from the literature that there is a tipping point where leakage of methane can cause the benefits of natural gas over coal to disappear, and that leakage in some regions has been observed to meet these levels [9]. As such, concerted efforts have been made to understand and reduce these emissions [10].

LDAR programs have gained prominence as a possible solution to reducing upstream fugitive emissions. LDAR programs involve site visits by trained operators who look for

emissions problems and either fix them or "tag" them for later repair. Preliminary work has suggested significant emissions savings could be achieved by going after fugitive emissions [11], and the International Energy Agency World Energy Outlook 2017 claims that 40 to 50% of oil and gas related methane emissions could be avoided at no net cost [12]. Following suit, new policies and government regulations have made LDAR programs mandatory in some areas [13]. All of this said, there has been limited quantitative work published showing the emissions reductions achieved by such LDAR programs, as "before and after" surveys are expensive and time consuming. Additionally, more studies need to be published on smart design of programs and surveys (e.g. LDAR frequency, survey breadth and depth). Smart LDAR design will ultimately depend on understanding the effectiveness of current LDAR programs and where their weaknesses lie.

To date, we know of one study that has been published on the persistence of emissions over time [14]. With this work, we aim to provide the building blocks for understanding LDAR survey effectiveness, filling in a vital gap that currently exists in the academic literature.

1.1.2 Life-cycle Assessment of Liquefied Natural Gas

In recent years, many papers have been published on the LCA impacts of Canadian and U.S. LNG exports [15, 16, 17]. These studies tend to follow the same general framework, accounting for and estimating emissions from the five stages we have defined for this analysis. This similar structure allows for relatively simple high-level comparisons between studies. In addition to academic studies, the literature contains numerous environmental impact assessments (EIAs) for proposed and operational LNG plants in a variety of countries including the U.S., Canada, and Australia.

More generally, a number of studies in the past decade have focused on assessing the upstream emissions impact of oil and natural gas production [18, 19]. Such studies have shown that upstream emissions can vary greatly depending on a multitude of factors, including field location, production characteristics, and operator. Together, these sources provided input data for our analysis and comparisons.

One key source is a report from the Canadian Institute of Resources Law that aggregated various data sources to estimate the life-cycle GHG emissions of Canadian LNG exports [15]. They found that life-cycle emissions benefits depended on LNG export destination, with LNG displacing different resources in different countries. They claim that China's domestic gas supply may not meet demand post-2020 without LNG imports, and that British Columbia (B.C.) LNG would have a lower emissions intensity than that of China's current power sector.

A study published by Abrahams et al. assessed GHG impacts of U.S. LNG exports to various countries, finding a mean intensity of 655 grams carbon dioxide-equivalent per kilowatt hour (g CO_2e/kWh) [16]. Shipping, re-gasification, and end-use emissions varied depending on import country. On average, they found U.S. LNG exports to be less emissions intensive than both Russian natural gas and average coal used for power generation and industrial heating (100-year global warming potentials (GWPs)).

Another recent study by Kusumu et al. echoed earlier results, and aggregated upstream and midstream data from 15 different studies focused on natural gas production [17]. Together with a National Energy Technology Laboratory (NETL) report on U.S. LNG, the team estimated life-cycle GHG emissions for Canadian LNG [20]. These results are used for comparison purposes below.

Lastly, reports exist focusing on B.C. LNG. Reports by the Delphi group (prepared for the B.C. Climate Action Secretariat), AECOM (prepared for Prince Rupert LNG Limited), the Kitimat LNG EIA, and the Pacific Northwest LNG EIA all provide additional information on expected GHG and air pollutant emissions from liquefaction processes [21, 22, 23, 24]. These reports differ from the academic literature in that they are 1) not peer-reviewed, and 2) generally rely on reported values or regulatory standards for emissions estimation. Nevertheless, they offer detailed engineering-design-based information on real-life liquefaction plants that have not previously been utilized in academic assessments of LNG.

Chapter 2

2 Methods

Our work can be broken down into two main areas: LDAR studies of 7G facilities, and LCA of the proposed 7G LNG project. As the LCA work relies on results from our LDAR work, the LDAR methods are presented first and the LCA methods are presented second.

2.1 Leak Detection and Repair Survey Effectiveness

As part of our work with 7G, we were given access to quarterly LDAR surveys performed by 7G contractors from 2015 to 2018. These quarterly surveys were completed for a portion of upstream production and processing sites in each visit. Site surveys were scheduled such that all of the sites operated by 7G were tested for leaks at least once a year. LDAR surveys began in late 2015 and have continued through present day. 7G used a single LDAR contractor, Davis Safety Ltd. (hereafter, Davis), to perform all surveys through end of 2017. In spring of 2018, 7G contracted with a different LDAR contractor. Our work analyzes only the surveys performed by Davis, allowing for better consistency in survey protocol, detail, and accuracy between different visits.

The goal of our LDAR analysis is two-fold, 1) to understand the fugitive emissions profiles of 7G upstream sites for purposes of the LCA, and 2) to assess and understand how leaks and vents behave over time when LDAR programs are in place. With respect to the second goal, a few key questions are of interest: (1) whether a leak that is fixed as a result of an LDAR survey stay fixed, and (2) whether a leak that is not fixed continues to leak over time. This information is valuable for planning frequency of LDAR surveys, as well as for simulating or assessing the potential costs and benefits of LDAR (e.g., cost of surveys, emissions reductions per unit of cost, etc.). To date, information on stability of leaks over time is difficult to obtain in the public literature because of the high cost of repeat surveys [25].

In order to assess the effects of LDAR through time, LDAR must be performed as repeated surveys of the same site. As surveys are expensive, such repeat LDAR data is limited. Among the 7G LDAR datasets, we have data for three sites that have been visited twice, and data for one site that has been visited three times. Data from 29 sites visited only once by Davis are not useful in the persistence analysis, but were valuable for estimating emissions profiles for the LCA work. 'Sites' here is a generic term that can refer to well pads (both "satellite" and "super pads"), processing plants, and compressor stations. Satellite pads are traditional well pads containing a small number of operating wells, while super pads are larger with more wells and have some gas processing equipment and tankage on-site. In 7G operations, super pads serve as gathering points for production from local satellite pads.

2.1.1 Leak and Vent Classification

We refer to all point source emissions of HCs detected during an LDAR survey as an emission source. Classifying each emission source as either a leak or vent provides more granularity on the kinds of sources prevalent at 7G sites. Leaks are unintentional emissions that do not occur by design – faulty equipment, operator error, or component wear and tear are all potential reasons for leaks. A vent is the opposite, being intentional to the way a piece of equipment operates. Examples of vents include emissions from gas-actuated pneumatic devices, or one-time events like well completions. From a GHG and volatile organic compound (VOC) emissions standpoint, both leaks and vents are important. That said, leaks can (normally) be easily repaired, whereas removing a vent may require a site redesign or the installation of additional equipment, such as a vapor recovery unit on a tank. In the 7G empirical LDAR dataset, leaks are regularly fixed between surveys, whereas vents are not. Table 2-1 outlines a subset of our determined categorization of Davis emissions sources into leaks and vents.

Table 2-1. Example sources of leaks and vents at upstream production and processing sites.

Leak Sources	Vent Sources
Threaded connection / flange	Gas-driven pneumatic valve
Thief hatch (corroded seal, left open accidentally)	Open ended line
Incomplete combustion (flare, combustor, engine)	Pressure safety valve
Pump / valve packing	Manifold / candy-cane vent

Davis surveyors noted whether an emission source was a leak or vent. Our reanalysis of the data found that some vent sources would be better classified as a leak. As such, the dataset was manually modified so that leak and vent classifications align with the description and distinctions in Table 2-1. In general, the classifications given by Davis are still largely used, and we only changed classification in a small number of cases. For example, we classified emissions from incomplete flare combustion as a leak, rather than a vent, as the ideal flare would combust all gas and not have incomplete combustion emissions of unoxidized HCs.

2.1.2 Survey Details

Davis performed quarterly surveys of 7G facilities between 2015 and 2017. Detailed component-level leakage surveys were conducted on production well pads, processing facilities, and compressor stations. Surveys took anywhere from half a day (for smaller satellite pads and compressor stations) to three days (for larger super pads and processing facilities). Survey length scaled with site complexity and component count. In the LDAR survey, Davis technicians examined every component and pipe using an optical-gas imaging (OGI) camera, the FLIR GF-320. Weather conditions were taken into account by calibrating a daily maximum observation distance from which the operator assessed components for leaks or vents. The daily maximum observation distance was defined as the distance at which a prescribed leak rate of 50-60 grams per hour (g/hr) of propane was viewable by the camera. However, weather conditions could change within a day, and the surveyor may or may not have adjusted survey behavior for such changes. Though surveys were completed largely by Davis, two Stanford University researchers (DJR-S and Arvind

Ravikumar) attended one week of LDAR surveys with Davis. Both researchers attest to Davis' methodological rigor and survey detail.

For each detected leak or vent, the LDAR crew recorded: location, description, component, RGB image of leaking component, infrared (IR) video of leak, and measured gas flow rate (assessed using a Hi-Flow sampler if the leak is accessible and safe). This level of granularity was useful for our persistence analysis, as it is important to know if a leak occurring in one visit is in fact the same leak occurring in the next visit.

An LDAR survey generally consists of three stages: leak detection, leak quantification (optional), and leak repair. Leak detection requires a technology that can detect methane, whereas quantification requires a technology that can measure gas flow rates for the desired gas species (primarily methane). The repair stage includes all maintenance activities required to stop the flow of gas from the system. Repair may also require the use of a methane-detecting technology to ensure that the repair is complete and effective (post-repair survey).

There are multiple technologies in use for LDAR, and many more in development. These surveys performed by Davis relied on a FLIR GF-320 OGI camera (Figure 2-1) for detection, and a Hi-Flow Sampler (Figure 2-2) for quantification.

The FLIR GF-320 camera operates in a spectral range of 3.2 – 3.4 micrometers (μm). Photons in this portion of the electromagnetic spectrum are easily absorbed to cause C-H bond ro-vibrational state changes. In contrast, IR photons outside of this narrow band (i.e., 3.0 or 3.5 μm) do not induce such changes and therefore are not absorbed by the gases with C-H bonds. Thus, a camera which can see photons in the 3.2 – 3.4 μm range is capable of visualizing methane, propane, butane, and hundreds of other HCs and VOCs with C-H bonds. The FLIR GF-320 relies on a cooled indium antimonide (InSb) detector, and is temperature calibrated to estimate object temperatures in the camera center field of view between -20° and 350° C.

The OGI camera is heavily reliant on the operator, as the camera visualizes gases but does not alert of their presence. It is the duty of the operator to spot the emissions plume via the

built-in screen. Small emission sources are difficult to spot, and thus the contractor skill level and the level of survey detail will ultimately determine the effective minimum detection limit of the camera. Furthermore, ambient conditions can also impair detection. Extremely hot temperatures may appear as emission sources, and snow or clouds can increase the difficulty of properly detecting a true emission source [26]. Surveys carried out by Davis regularly found emission sources that, when quantified, were below 0.2 g CH_4/min (0.01 cubic feet per minute, CFM).

The Hi-Flow Sampler relies on catalytic oxidation and thermal conductivity sensors to quantify emission sources that range from 0.01 to 10.50 CFM. Official Hi-Flow specifications states that it operates with an accuracy of ± 5% in a temperature range of 0° to 50° C. There are some doubts regarding the accuracy of the sampler, with a 2015 paper showing that sensor transition failure was routinely leading to underestimated emission rates in their tests, especially when gas streams contained large amounts of C_2 and higher HCs [27]. Regardless, the Hi-Flow Sampler is still the standard method for quantifying emission sources [28]. New technologies, such as quantitative OGI (qOGI) are in their infancy [29, 30].

Figure 2-1. FLIR GFx320 OGI camera (left) [31]*, and similar camera in use at the Methane Emissions Technology Evaluation Center (right)* [32].

Figure 2-2. Hi-Flow Sampler (left), and operator using the camera to quantify an emission point (right) [33].

2.1.3 Differences in Contractors

LDAR surveys using OGI cameras are highly dependent on the camera operator. Ongoing studies are attempting to quantify how much variation exists between contractors and what the impact may be on survey effectiveness and assumptions on resulting emissions reductions. 7G has used, occasionally, contractors other than Davis for LDAR surveys. In two cases, two contractors were used at the same site within a few months of one another. Figure 2-3 shows that Contractor A performed poorly compared to Contractor B (Davis). Contractor A completed surveys in April, and Davis completed follow-up surveys in June and July. Temporal and operational differences may explain some of the missed emission sources but cannot likely explain the differences in number of leaks found. These results are a key reason why we only use surveys performed by the same contractor in our analysis. Additionally, such differences raise an important consideration for regulators and policy-makers.

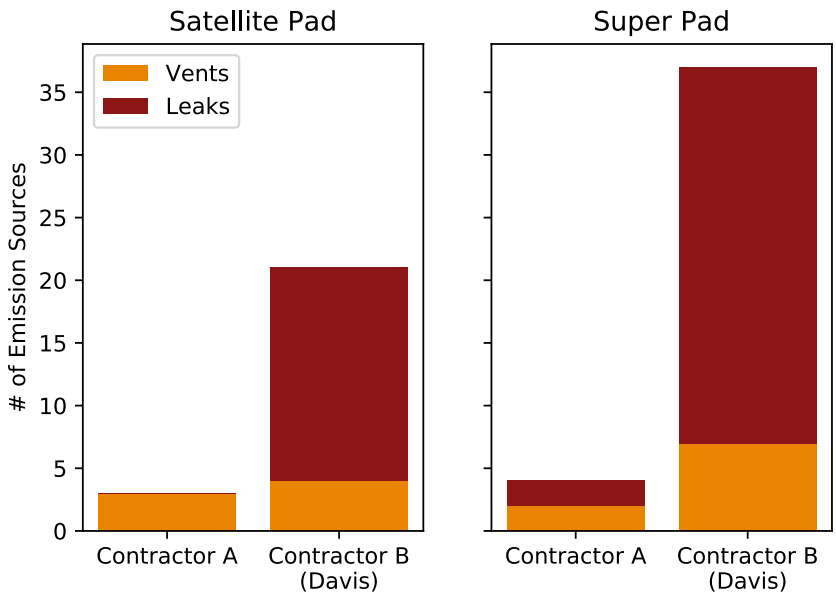

Figure 2-3. Differences in number of emissions sources found by two different LDAR survey contractors at the same sites. Satellite pad visited two months apart (left), and super pad visited three and a half months apart (right).

2.1.4 Supplementing Incomplete Data

Not all detected leaks and vents were quantified, as the Hi-Flow sampler requires that the emission point be within reach of the surveyor and safe to measure. For instance, tank emission points have never been quantified in any 7G survey. Other emissions, such as from overhead pipe racks, were also inaccessible. Rather than assigning these emission points a value of zero, we chose to supplement the empirical LDAR dataset and assign an estimated flow rate to these unquantified points. For tank-related emission sources, emission factors (EFs) from a database of measured tank emissions were applied. This database was compiled by Stanford University researcher Jacob Englander, and includes 613 unique tank-specific emission measurements, broken down by site-type, from a number of studies [11, 34, 35, 36, 37, 38, 39]. For non-tank-related emission sources, that were unquantified, we applied the average flow rate from leaks that were quantified. We use only initial surveys for determining these average flow rates, to better represent native leak volumes before any repair. See Table 2-2 for applied flow rates utilized in this work. The standard error of each mean flow rate is estimated as using:

$$\sigma_{\bar{x}} \approx \frac{s}{\sqrt{n}} \tag{2.1}$$

Where s is the sample standard deviation and n is the number of observations.

It is apparent from our analysis that the tank EFs applied are much larger than those found and measured from other emission sources. This is to be expected, as tanks are regularly recognized as the largest source of fugitive emissions [38]. Tank emissions result from accumulation of condensate liquids in the tanks. As the temperature of the condensate increases, gases vaporize from the condensate into the tank head space. Such gases either purposefully vent, escape due to an operator error (such as an open thief hatch), or force a leak (through corrosion or component fatigue). Looking at first visits for sites, we find that tank-related emissions account for 45% of total emissions while non-tank-related emissions account for the remainder (55%). This breakdown is skewed by a minority of sites that attribute a large amount of field-wide emissions to tanks, as demonstrated in Figure 2-4.

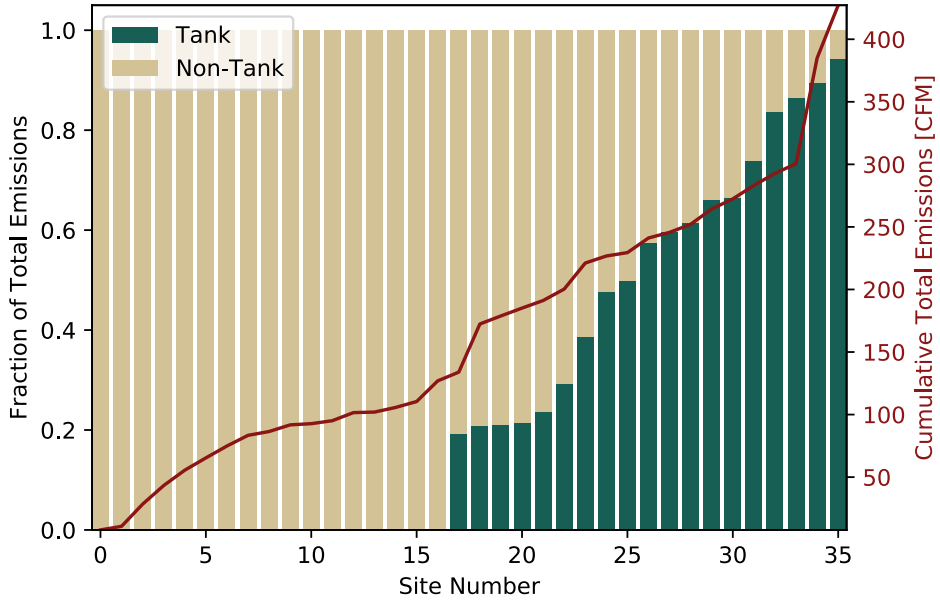

Figure 2-4. Fugitive emissions broken down by tank and non-tank emission sources, overlaid with cumulative emissions. Rank ordered by fraction of tank emissions.

In some cases, we needed to apply a flow rate for an unquantified emission source and found that emission type had not been previously quantified at that specific site type (e.g.

chemical injection pump at super pad, see Table 2-2). In these cases, the average flow rate from a similar site type was applied. Typically, this meant satellite pads and super pads were interchanged, and compressor stations, gas plants, and condensate plants were interchanged. The impacts of this decision were minimal, as there were fewer than five cases that required this substitution.

Table 2-2. Leak rates used for supplementing data. Shaded rows are factors taken from the leaking tank database, all other rows are from quantified emission sources in our dataset. No average flow rate is given if component was not quantified at that site type, and no standard error given if sample size was one.

Emission Source	Satellite Pad		Super Pad		Compressor Station		Gas Processing Plant		Condensate Plant	
	Avg. Flow Rate [CFM]	Standard Error [CFM]	Avg. Flow Rate [CFM]	Standard Error [CFM]	Avg. Flow Rate [CFM]	Standard Error [CFM]	Avg. Flow Rate [CFM]	Standard Error [CFM]	Avg. Flow Rate [CFM]	Standard Error [CFM]
Tank Level Indicator	1.34	0.13	1.34	0.13	1.42	0.78	3.98	3.00	3.98	3.00
Threaded Connection	0.05	0.01	0.04	0.01	0.04	0.01	0.06	0.03	0.03	0.01
Open Ended Line / Vent	0.62	0.13	0.22	0.06	0.56	0.16	0.12	0.08	0.25	0.07
Catadyne Heater	0.10	0.01	0.06	0.01	0.12	0.01	0.01	0.00	0.11	0.01
Flange Connection	0.10	0.09	0.01	0.00	0.04	0.02	0.02	0.01	0.04	0.00
Misc	0.07	0.06	0.07	-	0.05	0.02	0.01	0.00	0.06	0.02
Valve	0.07	0.02	0.04	0.01	0.04	0.02	0.01	0.00	0.41	0.26
Regulator	0.06	0.02	0.03	0.01	0.03	0.01	-	-	0.05	0.02
Compressor, Cylinder Head	-	-	0.12	0.04	-	-	-	-	0.11	0.08
Controller	0.17	0.03	0.15	0.05	0.09	0.06	-	-	0.18	-
Thief Hatch	1.34	0.13	1.34	0.13	1.42	0.78	3.98	3.00	3.98	3.00
Pressure Safety Valve (PSV)	0.25	-	0.20	-	-	-	-	-	-	-
Meter / Instrumentation	0.09	0.06	0.15	0.05	0.02	0.01	-	-	0.18	-
Tank PVRV	1.34	0.13	1.34	0.13	1.42	0.78	3.98	3.00	3.98	3.00
Pneumatic Pump	0.04	0.02	-	-	-	-	-	-	-	-
Other Tank	1.34	0.13	1.34	0.13	1.42	0.78	3.98	3.00	3.98	3.00
Chemical Injection Pump	0.17	0.08	-	-	0.02	0.01	-	-	-	-
Actuator	0.36	0.15	0.01	-	0.05	0.02	-	-	-	-
Analyzer	0.06	0.02	0.15	0.03	-	-	-	-	-	-
Engine (Including Fuel/Start Gas)	0.06	0.01	0.02	0.00	0.04	0.02	-	-	0.01	0.00
Pump Packing	0.11	0.07	0.01	-	-	-	-	-	-	-

2.1.5 Converting from Volume Flow to Mass Flow

Thus far, all emission rates have been presented as volumetric flow rates. In practice, emissions are most useful when expressed as a mass flow rate. Mass is a more useful metric than volume as it allows for the easy calculation of GHG equivalence (grams CO_2e), and for comparisons with the existing literature. Results for the LDAR work, as well as the LCA work, will present emissions as a mass flow rate of methane. Central to this conversion is the molar volume, which is calculated using the ideal gas law:

$$V_m = \frac{RT}{P} \tag{2.2}$$

We then use the following equation to calculate mass flow rate from volume flow rate:

$$\dot{m} = \frac{\dot{V} X_{CH_4} M_{CH_4}}{V_m} \tag{2.3}$$

Constants and variables used in Equations 2.2 and 2.3 are defined in Table 2-3. Volume flow rate traditionally has units of CFM, and mass flow rate traditionally has units of grams per second (g/s). Additional conversion constants are required to convert between these units. The mole fraction of CH_4 was taken as the average separator gas composition from 7G upstream production sites. We would expect to see some variability between individual sites with respect to this number.

Table 2-3. Constants and variables used in Equations 2.2 and 2.3.

Symbol	Definition	Value (if applicable)	Units
R	Gas constant	0.082057338	[L atm K^{-1} mol^{-1}]
T	Oilfield standard temperature	288.15	[K]
P	Oilfield standard pressure	1	[atm]
V_m	Molar volume at oilfield standard	23.64	[L mol^{-1}]
	Volume flow rate	-	-
X_{CH4}	Mole fraction of CH_4 in the gas stream	0.8078	[mol CH4 / mol gas]
M_{CH4}	Molecular weight of CH_4	16.04	[g mol^{-1}]
$\dot{m}$	Mass flow rate	-	-

2.1.6 Attempts to Normalize by Total Component Counts

A useful measure of a site's performance is the fraction of total components that are point source emitters. A large fraction would indicate a failing site with serious equipment fatigue and operational issues, whereas a small fraction would indicate a site that is operating as designed. In prior surveys, typical findings range from 0.1% to 1% of surveyed components leaking [34, 40]. To determine the fraction of leaking components, we need to know the number of emitting components and number of total components (activity factors) at the site, for each component type.

Knowing the number of components by component type would also allow for the development of component-level EFs, which are useful for emissions inventories. For example, the Environmental Protection Agency Greenhouse Gas Inventory relies on EFs and component counts to estimate emissions from the natural gas sector. An EF is applied to all components, not requiring knowledge of whether a component is leaking. EFs do not include an appropriate distribution of emissions, but they are used to get an aggregate estimate of overall emissions. The average flow rates we calculated earlier are applied to components that are emitting. Average leak flow rates will be orders of magnitude higher than EFs, due to the fact that only 0.1% to 1% of components are leaking in a typical case. EFs are calculated using Equation 2.4, whereas average flow rates are calculated using Equation 2.5.

$$EF = \frac{E_{total}}{N_{total}} \tag{2.4}$$

$$Avg.Flow\ Rate = \frac{E_{total}}{N_{leaking}} \tag{2.5}$$

Where E_{total} refers to total emissions, N_{total} refers to the total number of components, and $N_{leaking}$ refers to the total number of leaking components.

7G provided us with isometric diagrams for one super pad. We expected that using these diagrams we would be able to determine total component counts at each site, and align

these components with the component designations from LDAR surveys (those listed in Table 2-2). Unfortunately, we found that the level of detail in the isometric diagrams (flanges, valves, etc.) generally exceeded the level of granularity in the LDAR surveys (regulator, pneumatic pump, etc.). Table 2-4 lists the data from the raw site isometric diagram, in hopes that the component counts by equipment type will be useful in future work.

Table 2-4. Component counts for major equipment installations at an upstream production site.

Equipment Type	PIPE		FITTINGS		FLANGES		GASKETS		BOLTS		VALVES / IN-LINE		INSTRUMENTS	
	Count	% of Equip. Total	Count	% of Equip. Total	Count	% of Equip. Total	Count	% of Equip. Total	Count	% of Equip. Total	Count	% of Equip. Total	Count	% of Equip. Total
Module 1	49	10%	223	45%	66	13%	37	7%	42	8%	83	17%	0	0%
Module 2	42	9%	212	47%	58	13%	33	7%	38	8%	67	15%	0	0%
Module 3	61	10%	292	47%	88	14%	42	7%	53	9%	84	14%	0	0%
Module 4	45	10%	212	48%	52	12%	33	7%	38	9%	66	15%	0	0%
Module 5	23	7%	151	47%	40	12%	29	9%	29	9%	50	16%	0	0%
Module 6	17	43%	2	5%	17	43%	2	5%	2	5%	0	0%	0	0%
Module 7	42	9%	213	47%	61	14%	34	8%	38	8%	62	14%	0	0%
Module 8	33	8%	179	46%	52	13%	31	8%	34	9%	64	16%	0	0%
Module 9	10	9%	56	49%	11	10%	10	9%	10	9%	18	16%	0	0%
Booster Compressor 1	8	8%	48	50%	7	7%	7	7%	9	9%	17	18%	0	0%
Booster Compressor 2	8	8%	48	50%	7	7%	7	7%	9	9%	17	18%	0	0%
Compressor 1 & 2	44	8%	187	35%	60	11%	54	10%	83	15%	107	20%	2	0%
Lube Scrubber	5	11%	15	34%	5	11%	4	9%	6	14%	8	18%	1	2%
Condensate Pump Building	10	8%	55	45%	10	8%	10	8%	12	10%	24	20%	0	0%
Condensate Stabilization	46	9%	194	37%	53	10%	49	9%	63	12%	105	20%	10	2%
Condensate Stabilization - Flare	4	9%	16	36%	4	9%	8	18%	10	23%	2	5%	0	0%
Dehydrator 1 & 2	47	11%	158	37%	51	12%	40	9%	55	13%	74	17%	1	0%
Flare Area (High Pressure and Low Pressure)	20	8%	99	40%	38	15%	27	11%	31	13%	31	13%	1	0%
Gas Sweetening Unit 1	14	15%	28	29%	15	16%	12	13%	14	15%	13	14%	0	0%
Gas Sweetening Unit 2	8	11%	23	31%	12	16%	10	14%	12	16%	9	12%	0	0%
Genset	6	10%	23	38%	6	10%	7	11%	8	13%	10	16%	1	2%
Group Separator	11	14%	20	25%	13	16%	11	14%	14	18%	10	13%	0	0%
Heat Medium	4	11%	13	36%	4	11%	4	11%	4	11%	7	19%	0	0%
Instrument Air Compressor	1	11%	3	33%	1	11%	1	11%	1	11%	2	22%	0	0%
Interconnecting Pipes	39	10%	160	43%	46	12%	42	11%	44	12%	44	12%	1	0%
Risers	20	11%	86	46%	9	5%	9	5%	9	5%	54	29%	0	0%
Separator Package	36	16%	85	37%	42	18%	22	9%	22	9%	24	10%	1	0%
Condensate Tank	6	13%	14	30%	6	13%	6	13%	8	17%	6	13%	0	0%
Water Tank Farm	22	9%	91	37%	31	12%	26	10%	36	14%	41	16%	2	1%
Wellhead	1	4%	8	32%	3	12%	3	12%	3	12%	7	28%	0	0%

2.1.7 Persistence Analysis

To assess emissions persistence and continuity of leaks and vents over time, we designated three categories that an emission point could be categorized into during the initial survey, and five categories for the repeat surveys. Categories and descriptions are in Table 2-5. Placing emission points into these categories allowed us to determine the effectiveness and benefits derived from these LDAR surveys.

Table 2-5. Categories for emission points found during initial survey and resurveys.

Initial Survey		Resurvey	
Category	**Description**	**Category**	**Description**
Leak, Fixed	Leak found in the initial survey, and fixed at some point between the initial and resurvey	Leak, Fixed	Leak fixed after the initial survey that has reappeared in the resurvey
Leak, Not Fixed	Leak found in the initial survey, with no action made to fix it before the resurvey	Leak, Not Fixed	Leak not fixed after the initial survey that has persisted until the resurvey
Vent	Vent found in the initial survey	Vent	Vent found in the initial survey and the resurvey
		New Leak	Leak that was not found in the initial survey
		New Vent	Vent that was not found in the initial survey

As vents are intentional and part of system design, we do not observe any cases where a vent is fixed after the initial survey. As such, we would expect to see all vents from the initial survey in the resurvey. Due to the periodic nature of some vents, it is possible for a vent to be found in one survey and not the other. This is one contributor to the new vent category for resurveys. Another contributor is equipment changes or site expansions that add new vents to a site.

Placing emission points into these categories was a manually intensive process. Categorizing the initial surveys was straight forward, as we had already classified each point source as either a leak or vent, and the dataset reported whether a leak had been fixed or not. The difficulty is in categorizing the resurveys, as we had to manually determine whether a leak or vent found in the resurvey was present in the initial survey.

The process to manually determine whether a leak was repeatedly found in subsequent surveys is as follows:

1. Photos and videos of the emitting equipment (from both surveys) were examined;

2. Emission point locations and descriptions were examined;

3. Descriptions that are not standardized are examined for slight changes in terminology that would likely indicate a similar source;

Challenges arose due to changes in ambient conditions between surveys, such as snow, and differing camera angles and zoom levels. In some cases, this made it difficult to compare photos and videos. Despite difficulties, utilizing the breadth of data reported in these surveys made it unambiguous in most cases whether an emission point was previously existing or new.

2.2 Life-cycle Assessment of Liquefied Natural Gas

The LCA portion of our study used operational data provided by 7G, and academic studies, government reports and EIAs of existing LNG facilities. In addition, we used OPGEE to analyze upstream production-related emissions.

2.2.1 Case Definitions

All cases involve natural gas produced in Northern Alberta within the Montney basin, shipped to coastal B.C., and liquefied for transport to Shenzhen City in the Guangdong Province of China. See Figure 2-5 for an illustration of the system boundary.

To allow for meaningful comparisons between the three LCAs by the participating teams from University of Calgary, Stanford University, and University of British Columbia, all teams agreed on a common base case scenario and set of underlying base case assumptions. This base case represents a conservative estimate of emissions associated with the proposed LNG project. All cases use lower heating value (LHV) for engineering calculations and therefore report LHV efficiencies and GHG intensities. Climate impacts are assessed using 100-year GWP values from the IPCC AR4 report [41]. The base case scenario assumptions, as well variants explored as additional scenarios, are outlined in Table 2-6.

The base case LNG project scale is assumed to produce 1 bcf/d of LNG (i.e., 1 bcf/d net of self-consumption in liquefied form before loading onto the transport ship). The base case requires lead-time to permit and construct the liquefaction plant and required pipelines to B.C., as well as time to increase upstream production to meet the demand of the LNG plant. Current 7G operations produce approximately 450 million standard cubic feet per day (mmscf/d) of raw gas. In the base case, liquefaction of 1 bcf/d gas will begin in June of 2022.

Figure 2-5. Base case natural gas production, liquefaction, and end-use locations.

Table 2-6. Base case assumptions (left) and alternative case assumptions examined in additional scenarios.

Stage	Base Case	Additional Scenarios
Upstream	• Model of expected 7G operations to produce 1 Bcf/d, modeled as an expansion of current operations.	None
Midstream	• Transmission from Grande Prairie to B.C. coast using 7 compressor stations (4 NG, 3 electric). • Pre-treatment for liquefaction via simple-cycle natural gas combustion turbine (NGCT) at 40% efficiency.	None
Liquefaction	• Liquefaction power generation and compression via natural gas combined cycle (NGCC) operating at 54% efficiency.	• NGCC for compression, low-carbon electricity from B.C. Hydro for power generation. • Low-carbon electricity from B.C. Hydro for compression and power generation. • Simple-cycle NGCT at 39% efficiency.
Transport	• Shipping from B.C. to Shenzhen via ocean taker using boil-off gas (BOG) and additional regasification. Return trip using diesel. • Re-gasification with no emissions savings from using cooling potential.	• Shipping return trip with bunker fuel.
Downstream	• 30km transmission to either power generation plant or district heating. • Power generation via 54% efficient NGCC, or district heating at 85% efficiency.	• Power generation via 48% efficient NGCC (high emissions). • Power generation via 60% efficient NGCC (low emissions).

2.2.2 System Boundaries and Allocation

We performed a bottom-up engineering-based LCA to model emissions across the project value chain. We utilized a variety of data streams and modeling tools. Figure 2-6 shows an overview of the mass flows of gas and condensate for our base case

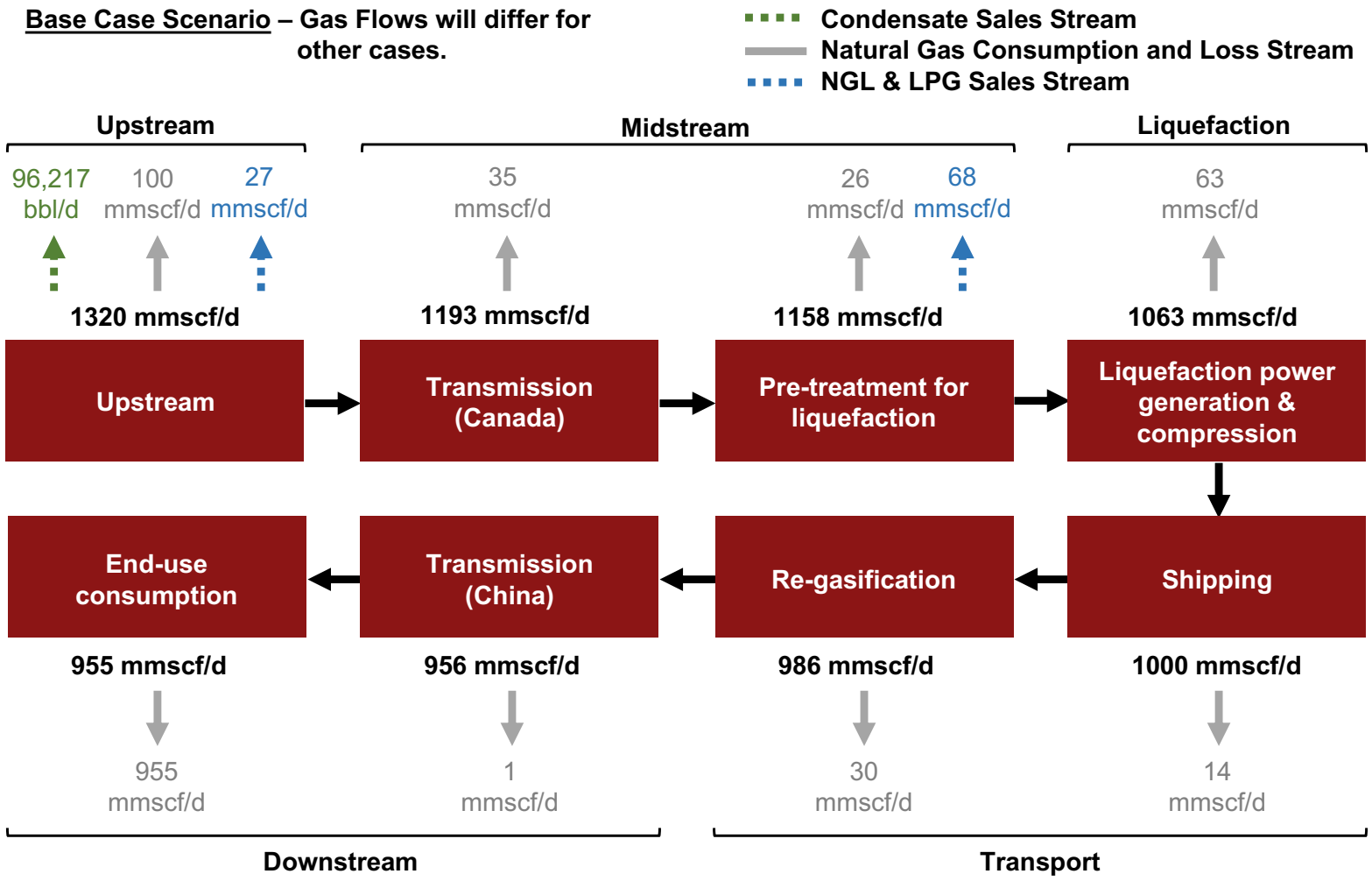

Figure 2-6. Disposition of original condensate and gas production. Base case condensate and raw gas production is 96,217 bbl/d and 1,320 mmscf/d, with end-use consumption of 955 mmscf/d at the power generation station or district heating system. For clarity, this diagram does not include external energy flows into the system even when they are counted in the GHG assessment (e.g., bunker fuel consumed on ship).

7G is a liquids-rich natural gas producer, so their upstream operations produce lease condensate, light HCs (liquefied petroleum gas (LPG) or natural gas liquids (NGLs)), and natural gas. A common challenge in LCA is the question of how to assign emissions when a single facility produces a variety of products (so-called "co-production"). LCA methods allow a variety of means to allocate total operational emissions to each co-product.

The most commonly-applied method of handling co-production is to divide or allocate the total emissions from a facility or project to the different co-products (called "allocation" in the LCA literature). Another set of methods assumes "displacement" of one of the products. In displacement-based methods, all emissions from the facility are counted after which emissions from the co-products or byproducts are subtracted from the total by assuming that the co-product displaces a similar product from another facility or process.

In this study, we use allocation to divide emissions between the produced gas and other products. Different denominating qualities are used in allocating emissions to different end products. Previously developed methods use energy content, mass content, or economic value of the multiple products. For energy systems LCA, the most common method is to allocate emissions to products based on share of energy content in the resulting co-products (e.g., if natural gas contains half of the energy produced at a facility, it is assigned half of the total emissions).

For the upstream portion of our base case analysis, 70% of emissions are attributed to natural gas, with the rest attributed to condensate and NGL/LPG. Note that current 7G operations have a lower energy share of 60% of the produced energy content as gas due to higher liquids production compared to expected operation in 2022. Modeling of expanded production from 7G sites suggests that the ratio of gas to liquids production (gas-oil ratio, GOR) will increase over time, such that more gas will be produced per unit liquids than in current operations.

For midstream allocation at the point of LPG separation, 86% of emissions are allocated to the LNG stream and the remainder of midstream emissions (14%) are allocated to LPG produced at the final ("deep cut") separation stage prior to liquefaction. Emissions from

liquefaction, shipping, and downstream combustion are attributed fully to gas, as no further liquids are extracted from the methane-rich gas stream that enters the liquefaction train.

2.2.3 Upstream

Upstream emissions, though small in comparison to downstream end-use emissions, are an important source of variability in the life-cycle emissions of oil and gas. The complexity and scale of upstream operations, as well as the level-of-control over operations that producers have, make upstream emissions a prime target for reduction efforts. As such, a disproportionately large amount of work (in reference to share of emissions) was put into assessing upstream impacts.

2.2.3.1 Decline Curve Analysis

Hydraulically fractured wells typically exhibit rapid productivity declines in the first year or two of production. After this period of initial rapid decline, the decline rate slows and production persist for years in a "long tail" production behavior. This pattern has been widely documented in unconventional shale and tight plays, across a variety of basins. In order to model this production pattern, two key models are used in the literature: stretched exponential (SE) and hyperbolic decline (HD) models [42].

The SE model is defined as:

$$q(t) = q_0 \exp\left[-\left(\frac{t}{\tau}\right)^n\right] \tag{2.6}$$

And the HD model is defined as:

$$q(t) = \frac{q_0}{(1 + bDt)^{1/b}} \tag{2.7}$$

Where $q(t)$ is production in month t, q_0 is initial monthly production, t is time in months, and τ, n, b, and D are all fitting parameters.

We obtained “type curves” from 7G for production from the “Nest 2” type geology. These type curves show production decline by averaging a number of real-world production profiles (i.e., they are indicative and not representative of any particular well). These type curves are fit to SE and HD models. As the models both have the same number of degrees of freedom (3 variables in each), we pick the model with the least root mean square error (RMSE) when fitting the type curve. The best fitting model to 7G type curves is the SE model. The resulting fits, fitting parameter values, and RMSE are presented in Figure 2-7. Using these fits, we design a drilling program from 2017 through 2052 to achieve production requirements of 1 bcf/d gas-to-LNG.

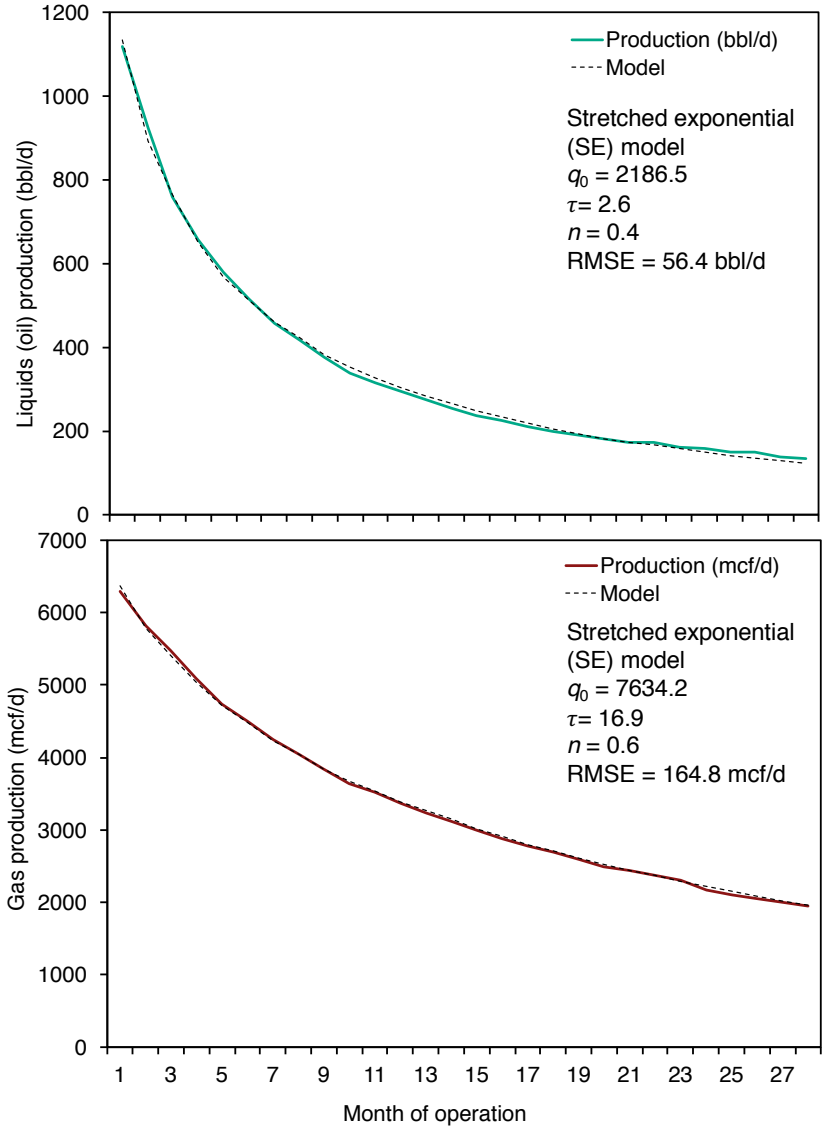

Figure 2-7. 7G "type curves" for oil (top) and gas (bottom) production from Nest 2 geological play. Best fitting SE models presented as dashed lines with fitting parameters and RMSE listed.

The drilling plan for the 7G project is assumed to include drilling a number of identical Nest 2 wells in each month until production stabilizes at the desired rate. We assume a lifetime of 20 years per well, at which point the production is deemed too low to continue operation for economic purposes and the well is subsequently shut-in and plugged. The desired rate of gas production is increased by 5% to account for inevitable well downtime including maintenance and repairs (i.e., for desired production of 100 mmscf/d, wells should have a capacity of 105 mmscf/d). Required base case raw gas production should be approximately 1,320 bcf/d (see Figure 2-6). This amount allows for fugitive losses,

condensation and fractionation of liquids and LPG, as well as gas consumption in production, processing, transmission, and liquefaction.

A monthly drilling plan is devised so that production reaches the desired target by June of 2022 and remains at or above the target level until 30 years later (June 2052). This drilling plan calls for 113 wells drilled per year in 2017-2022 (~9.5 per month), 87 wells drilled per year in 2022-2031, and 86 wells drilled per year in 2031-2052. This drilling plan and resulting gas production is presented in Figure 2-8. Due to more rapid liquids decline than gas decline, the GOR increases from approximately 7,300 to >13,500 standard cubic feet per barrel (scf/bbl) over the project lifetime. This change requires the number of wells drilled per year to decline over the life of the project and explains the increase in gas-attributed emissions from an energy allocation.

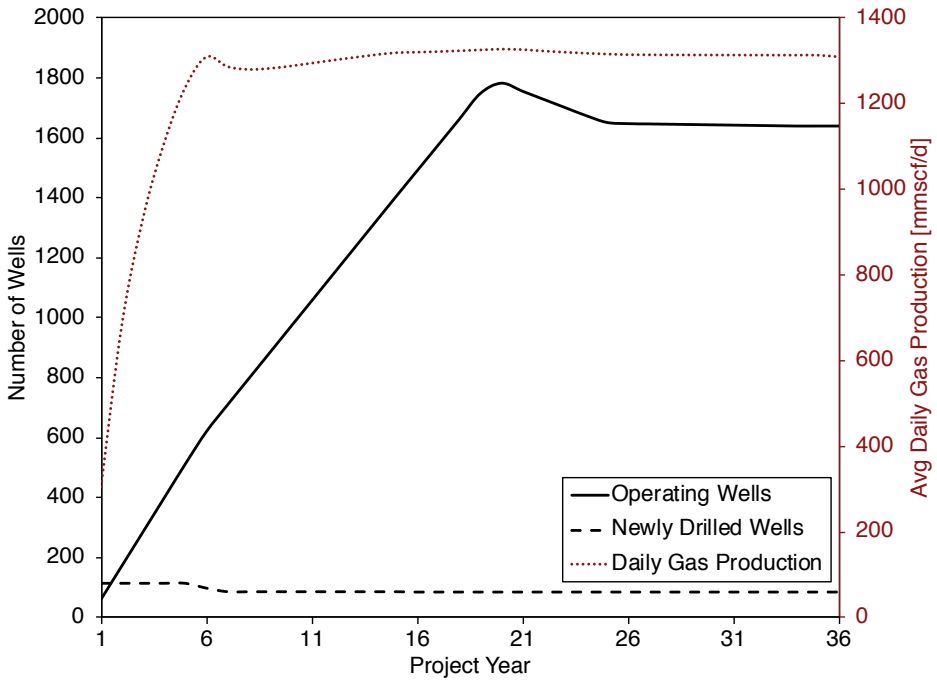

Figure 2-8. 7G drilling plan (left axis) and subsequent gas production (right axis).

2.2.3.2 Oil Production Greenhouse Gas Emissions Estimator (OPGEE)

We use OPGEE to estimate upstream GHG emissions associated with 7G operations. OPGEE estimates the life-cycle GHG emissions associated with the production, processing, and transmission of oil and gas products. Detailed documentation and OPGEE

model files are available for free download [5]. Though OPGEE was traditionally built to assess the impacts of crude oil production, recent updates can assess impacts associated with gas production. For this analysis we use a version of OPGEE 3.0 that was undergoing development, though fully functional.

OPGEE relies on user inputs, literature assumptions, and engineering calculations to estimate total emissions. A user will enter parameter values in the input worksheet, while process stage and supplementary worksheets carry out calculations. Results are aggregated in the "GHG Emissions" (t CO_2e/d), "Energy Consumption" (mmbtu/d), and "Results" (g CO_2e/MJ) sheets. Figure 2-9 illustrates the general scope and structure of OPGEE 2.0, which has been expanded on in OPGEE 3.0 (gas transmission).

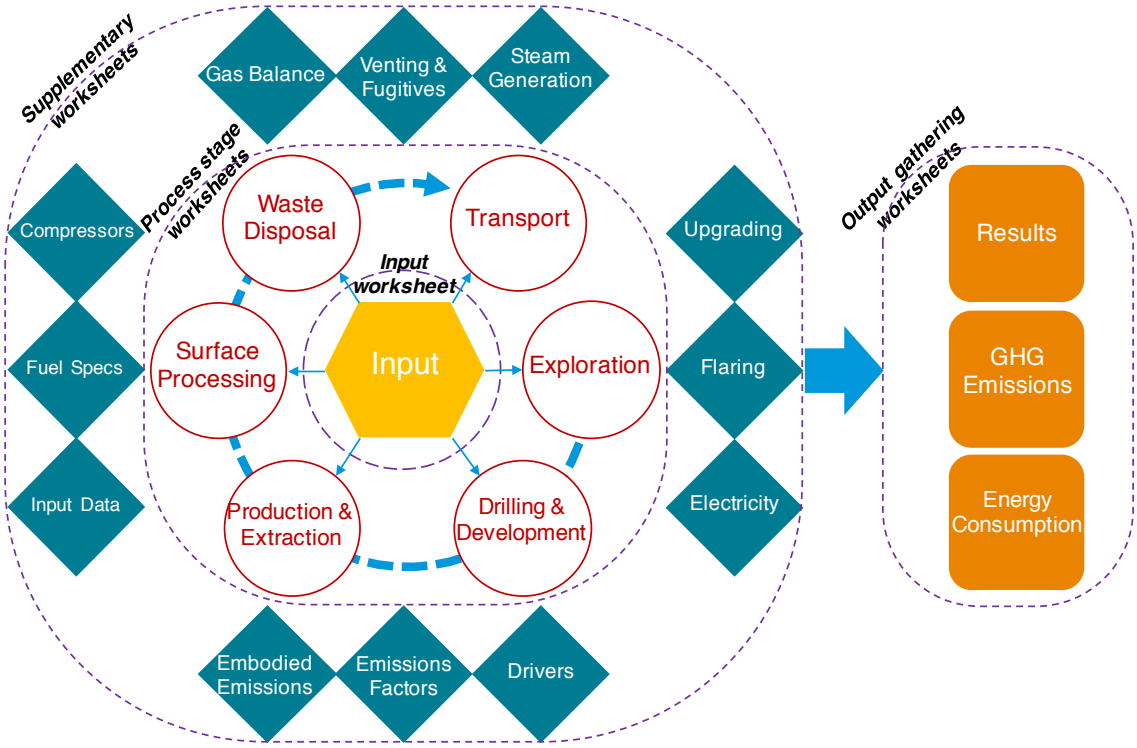

Figure 2-9. Structure of OPGEE 2.0. The version of OPGEE used in this analysis contains additional worksheets that allow for more specific modeling of gas processing. Graphic courtesy of Dr. Mohammad Masnadi [43].

OPGEE does not require all data inputs in order to run. If an input is not given, a "smart default" is used. Table 2-7 lists major inputs to OPGEE, categorized as either primary, secondary, or tertiary depending on importance to overall result. In addition to these inputs,

individual sheets in OPGEE allow the user to change assumptions and input additional, more-specific, inputs.

Table 2-7. OPGEE simplified input parameters. Primary in green, secondary in blue, and tertiary in black. Courtesy of Dr. Mohammad Masnadi [43].

Parameter	Unit
Production practice (e.g. downhole pump, injection, flooding, etc.)	[]
Field country	[]
Field age	year
Field depth	ft
Oil volumetric production	bbl/d
Number of producing wells	[]
Number of injection wells	[]
Well diameter	in
Productivity index	bbl/psi-d
Reservoir pressure	psi
Reservoir temperature	°F
API gravity	°API
Produced gas composition (N2, CO2, C1, C2, C3, C4+, H2S)	mol %
Gas-oil-ratio (GOR)	scf gas/bbl oil
Water-oil-ratio (WOR)	bbl water/bbl oil
Water injection ratio	bbl water/bbl oil
Gas lifting injection ratio	scf gas/bbl oil
Steam-oil-ratio (SOR)	bbl steam/bbl oil
Fraction of required electricity generated on-site	[]
Fraction of remaining natural gas reinjected	[]
Fraction of remaining water reinjected	[]
Fraction of steam generation via cogeneration	[]
Processing practice method (e.g. heater, stabilizer column, upgrader type, etc.)	[]
Flaring-oil-ratio (FOR)	scf/bbl oil
Venting-oil-ratio	scf/bbl oil
Land use impacts	[]
Crude oil transportation mean (e.g. ocean tanker, barge, pipeline, etc.)	[]

To determine emissions intensity of upstream operations, we use OPGEE to model emissions from 2017 through 2052. This is done by modeling each year independently, changing inputs for oil production volume, number of producing wells, and GOR based on our decline curve analysis. Our base case emissions intensity uses the average emissions intensity of the last six years of the project, values which are near steady-state. Emissions intensity outputs from OPGEE decrease over time, due to economy-of-scale benefits in

embodied emissions and drilling and development, and reduced surface processing emissions from changes in GOR. We examine how emissions intensity changes over time in the Results section.

For this study, we also added criteria air pollutants (CAPs) analysis to OPGEE in addition to the default GHGs. EFs were adapted from the greenhouse gases, regulated emissions, and energy use in transportation (GREET) Model to calculate emissions from combustion processes [44]. As CAPs other than VOCs are not present in fugitive emissions, we only need to account for emissions associated with combustion to account for the vast majority of CAP emissions. We apply GREET CAP EFs for combustion processes in OPGEE and throughout our analysis. GREET EFs are presented in Table 2-8.

Table 2-8. GREET EFs by fuel, equipment, and pollutant type that are utilized in OPGEE and our analysis [44].

Fuel Type	Equipment Type	Greenhouse Gases [g/mmbtu fuel]						Critera Air Pollutants [g/mmbtu fuel]					
		VOC	CO	CH_4	N_2O	CO_2	CO_2e	NOx	SOx	PM_{10}	$PM_{2.5}$	BC	OC
Natural Gas	Utility/ Industrial Boiler (>100 MMBtu/hr input)	2.54	22.21	1.06	0.75	59367	59660	36.40	0.27	3.51	3.51	0.58	1.50
	Small Industrial Boiler (10-100 MMBtu/hr input)	2.54	24.97	1.06	0.35	59363	59541	41.05	0.27	3.51	3.51	0.58	1.50
	Large Gas Turbine	1.06	41.29	1.06	0.10	59342	59468	31.97	0.27	3.58	3.58	0.10	2.43
	CC Gas Turbine	0.27	14.53	1.14	0.12	59386	59474	17.43	0.27	0.13	0.13	0.00	0.09
	Small Turbine	1.06	41.29	1.06	0.10	59342	59468	31.97	0.27	3.58	3.58	0.10	2.43
	Stationary Reciprocating Engine	133.32	705.99	392.35	0.11	56809	68194	832.95	0.27	7.20	7.20	1.44	3.08
	Ocean Tanker	79.91	90.80	91.62	2.00	58769	62048	2085.24	0.27	18.12	16.68	2.50	6.50
Diesel Fuel	Industrial Boiler	0.80	20.87	0.20	0.92	78163	78478	53.86	0.54	8.12	5.47	0.55	1.37
	Commercial Boiler	1.20	25.12	0.76	0.92	78154	78490	66.54	0.54	8.40	7.52	0.75	1.88
	Stationary Reciprocating Engine	2.03	657.01	4.22	0.60	77149	78491	2076.99	0.54	54.61	54.04	43.94	9.78
	Turbine	0.26	1.56	3.02	0.60	78187	78446	256.41	0.54	25.94	6.57	0.66	1.64
	Ocean Tanker	79.91	181.60	4.58	2.00	77652	78901	2085.24	0.54	181.21	166.75	25.01	65.03
Crude	Industrial Boiler	0.82	23.74	0.36	2.00	72932	73577	181.60	395.46	29.71	19.31	0.56	0.41
Residual oil	Industrial Boiler	0.91	36.02	3.23	1.71	85013	85664	137.08	683.33	35.35	16.17	1.03	0.71
Pet. Coke	Industrial Boiler	0.47	23.95	1.25	0.86	106933	107260	121.63	544.40	2.66	2.52	0.11	0.20
Coal	Industrial Boiler	0.47	23.95	1.25	0.86	100002	100328	121.63	544.40	2.66	2.52	0.11	0.20
Upgrader process gas	Stationary Reciprocating Engine	133.32	705.99	392.35	0.11	56809	68194	832.95	0.27	7.20	7.20	1.44	3.08
NGL	Diluent combustion	2.50	26.00	49.00	1.10	64820	66422	48.90	67.49	3.70	3.70	3.52	0.19
Gasoline	Stationary Reciprocating Engine	598.35	1520.44	3.00	0.60	72577	77118	98.59	1.24	52.56	52.56	5.26	16.82
Bunker Fuel	Ocean Tanker	79.91	181.60	4.58	2.00	84534	85783	2085.24	1443.57	181.21	166.75	25.01	65.03

In addition to including CAPs, we modified a number of OPGEE default assumptions to better match 7G production practices. Changes to the default OPGEE routine are presented in Table 2-9. All changes are based on internal documents shared by 7G. OPGEE-default assumptions that aligned well with 7G operational data are not highlighted in this table, as only changes to model defaults are explicitly tracked.

Availability of 7G-specific operational data allowed us to model sections of upstream production outside of OPGEE or allowed for project-specific data to be used in place of default assumptions. For example, the regular LDAR surveys at production sites allowed for fugitive methane emissions to be assessed separately. Similarly, granular land use data were used instead of default OPGEE assumptions. Furthermore, upstream processes not included in OPGEE like office heating, cooling, and electricity emissions, field maintenance trucks, and water handling operations were modeled independently.

Table 2-9. Adjusted default OPGEE assumptions.

Worksheet	Adjusted Metric	Default Value	New Value	Unit	Notes
Drilling & Development	Hole size	Medium	Extra-large	[-]	
	Fraction of wells horizontal	0.0	1.0	[-]	
	Length of lateral	5000	9800	[ft]	
	Fraction of wells fractured	0.0	1.0	[-]	
	Fracturing fluid injection volume	3.00	9.25	[million gallons]	
	Fracturing pressure gradient	0.70	0.80	[psi/ft]	
	Cumulative production per well	800000	411520	[bbl/well]	1
Flaring	Flaring efficiency	95%	98%	[-]	
Glycol Dehydrator	Model of dehyrdation used	Process sim stat approach	Textbook treatment	[-]	2
Demethanizer	Fraction of gas to demethanizer product streams				3
	C_2H_6	0.90	0.00	[-]	
	C_3H_8	0.99	0.20	[-]	
	C_4H_{10}	0.99	0.45	[-]	
Electricity Gen and Imports	Electricity import GHG emissions	160844	278416	[g CO_2e/mmbtu]	4
Embodied Emissions	Include embodied emissions?	No	Yes	[-]	
	Embodied emissions database	Ecoinvent	GREET	[-]	
	Are production wells fractured?	No	Yes	[-]	
	Shipment distance				
	Steel	1000	2100	[mi]	
	Cement	100	350	[mi]	
	Fracturing sand	1000	1500	[mi]	
	Shipment mode for cement	Truck	Rail	[-]	

[1] Adjusted based on provided type curve and decline curve analysis

[2] Textbook treatment relies on engineering calculations and was providing more reasonable estimates than other approach

[3] Adjusted to match 7G material balance sheet for upstream processing of gas

[4] Changed to Alberta default grid intensity factor

2.2.3.3 Fugitive Emissions

We utilized company-specific LDAR results to model fugitive emissions and vents from 7G operations. Proportional loss rate (PLR) is a measure commonly used to assess and compare site, field, and operator performance. We use it to estimate emissions for those sites that were not directly measured in an LDAR survey. PLR is defined as follows:

$$PLR = \frac{E_{CH_4}}{P_{NG} X_{CH_4}} \tag{2.8}$$

Where E_{CH4} is the volume of methane emissions from a site over some time period (determined from LDAR survey), P_{NG} is the total volume of gas production from that site over the same time period, and X_{CH4} is the molar concentration of methane in the produced gas.

We found a negative relationship between PLR and production for visited sites, as shown in Figure 10. This relationship is approximately linear in log-transformed PLR and log-transformed production volume. PLR is the fraction of gross gas production at a site lost to the air through leaks and vents. For sites that have not been visited during the study period, a PLR is estimated using this relationship and 2016 gas production. Fugitive emissions were then allocated to the three co-products and scaled-up to base case production levels assuming a linear increase in leakage with production.

The best fit equation for the line fit in Figure 2-10, with proportional loss rate *PLR* [%] and gas production P_{NG} [mmscf/d], is:

$$\ln(PLR) = -1.218 \cdot \ln(P_{NG}) + 8.554 \tag{2.9}$$

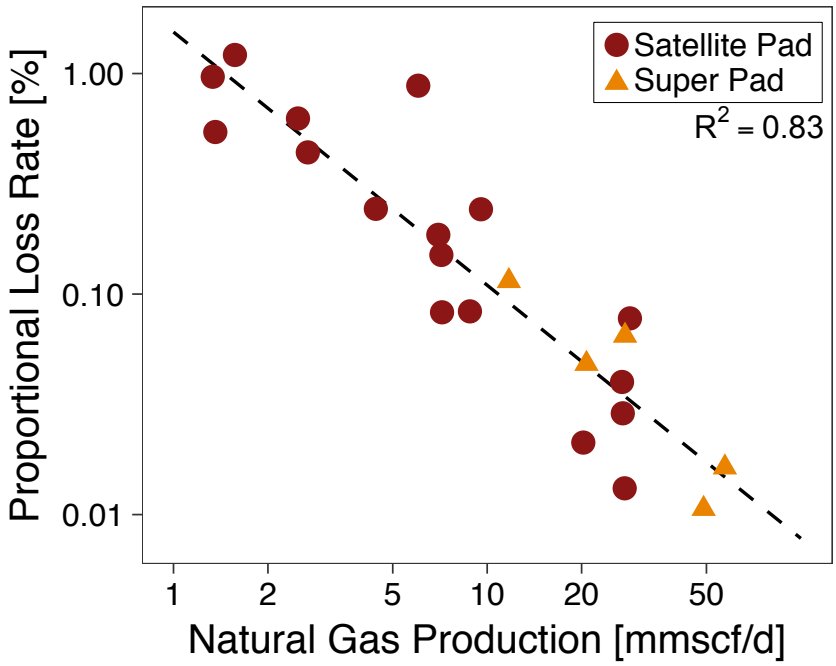

Figure 2-10. PLR decreases linearly with increasing natural gas production on a log-log basis.

2.2.3.4 Land Use Emissions

Land use impacts depend on the amount of land impacted and the carbon emissions per unit of land impacted. We discuss these elements separately below, for both upstream and midstream portions of our analysis.

Land impacted

Land-use data from 7G for existing production levels are scaled to 1 bcf/d production using linear extrapolation. Current upstream land use is taken as the summed reclamation area of all production sites, processing plants and compressor stations, access roads, housing structures, and storage areas. This area is multiplied by the scale-up factor to approximate future upstream land use area. Midstream land use refers to area occupied by a pipeline from Grande Prairie to coastal B.C., assumed to be 1100 km in length. A right-of-way of 70 meters for the pipeline is adopted based on the on TransCanada environmental impact analysis documents [45].

Carbon emissions per unit of land impacted

Upon land clearing, CO_2 emissions can arise from three sources:

1. Soils can release CO_2 through oxidation of fixed soil carbon caused by soil degradation, soil disturbance, tilling and scraping, and draining of moist soils.
2. Above-ground biomass is removed and can result in CO_2 emissions if the carbon contained is oxidized through burning, degradation and decay. If the wood is used for productive purposes, the carbon content of the wood can be stored rather than oxidized.
3. "Foregone sequestration" can result if an ecosystem that was actively storing carbon is disturbed.

Yeh et al. previously estimated land-associated CO_2 impacts of energy development in Alberta, and we adapt their basic approach to the current analysis [46].

Soil carbon uses assumptions of Yeh et al. (p. S6 [46]). For 30 cm soil disturbance, fractional loss of soil carbon is 0.3 (p. S8 [46]). Given 100 tonne/ha soil carbon content, this totals 30 tonnes/ha disturbed.

The area of forest land in Canada was obtained by consulting Canada's National Forest Inventory [47]. We collected data on 1000 ha of forest land by type and age class, (Table 5.0 [47]), above-ground biomass in million tonnes for four types of land cover (Table 17.1 [47]), and coverage in 1000s of Ha for the same four types of land cover (Table 5.1 [47]). Data are reported per terrestrial ecozone and per age class. Fraction of carbon in biomass is computed by ratio of carbon biomass (Table 19.1 [47]) to total biomass (Table 17.1 [47]). Each ecoregion and land cover type is converted to a single above-ground biomass value by weighting by reported area shares in each age class. Each above-ground biomass value is converted to carbon content, in tonne C/ha. See Table 2-10 for details.

Assuming the development occurs in a representative mixture of the three ecozones (Boreal Plain, Pacific Maritime, Montane Cordillera), the amount of carbon in each zone is 45.7, 137.3, and 80.0 tonnes C/ha. Upstream development is assumed to occur completely in

Boreal Plain region, while midstream development occurs in 70% Montane Cordillera and 30% Pacific Maritime. Thus, the carbon intensity (CI) of upstream development is 45.6 tonne C/ha, while pipeline development is 97.2 tonne C/ha.

Table 2-10. Above-ground biomass computed values by ecozone and land cover type. Data from Canada's National Forest Inventory.

Ecozone	Land Cover Type	Above-ground biomass [tonne/ha]	Area fraction of ecozone landscape	Weighted biomass [tonne/ha]	Weighted carbon [tonne/ha]
Boreal Plains	Non-treed	7.1	5.50%	-	-
Boreal Plains	Broadleaf	96.6	27.00%	-	-
Boreal Plains	Coniferous	65.8	55.20%	-	-
Boreal Plains	Mixedwood	106.8	12.30%	-	-
Boreal Plains	***Total***	**-**	**-**	***76.0***	***45.7***
Pacific Maritime	Non-treed	6.2	6.70%	-	-
Pacific Maritime	Broadleaf	156.9	2.60%	-	-
Pacific Maritime	Coniferous	295	88.20%	-	-
Pacific Maritime	Mixedwood	209.2	2.50%	-	-
Pacific Maritime	***Total***	**-**	**-**	***269.9***	***137.3***
Montane Cordillera	Non-treed	6.2	3.90%	-	-
Montane Cordillera	Broadleaf	110.2	2.40%	-	-
Montane Cordillera	Coniferous	165	88.80%	-	-
Montane Cordillera	Mixedwood	138.7	4.90%	-	-
Montane Cordillera	***Total***	**-**	**-**	***156.2***	***80.0***

Foregone sequestration is estimated at 0.04 tonne C/ha-yr for coniferous, 0.04 tonne C/ha-yr for broadleaf forest, and 0.77 tonne C/ha-yr for bogs/fens/peat zones (p. S9 [46]). Given forest cover in these regions is mostly coniferous, we estimate a 2 tonne C/ha foregone sequestration for a conservative 50-year disturbance time. Total CO_2 releases for upstream and midstream development are given in Table 2-11.

Table 2-11. Summary land use emissions computed for analysis, unallocated.

Stage	Land disturbed [ha]	Carbon per unit land [tonne C/ha]				Total emissions [tonne CO_2]
		Soil carbon	Above-ground loss	Foregone sequestration	Total	
Upstream	4856	30	45.7	2	77.65	1381651
Midstream	7700	30	97.2	2	129.2	3645284
Total	***12556***	**-**	**-**	**-**	**-**	***5026935***

2.2.3.5 Other Emission Sources

Finally, minor energy uses including office heating, cooling, and electricity for 2016 was supplied by 7G. An Alberta-specific electric grid consumption intensity was used [48]. To account for emissions from maintenance vehicles in upstream operations, we use data from 7G Carbon Disclosure Project reporting and typical assumptions on vehicle type and fuel [49]. Lastly, we estimate water handling using a 7G-provided factor of 17 L diesel consumption per m^3 of produced water [50]. All values were scaled linearly from 2016 data to calculate expected base case emissions (approximately 3x scaling factor).

2.2.4 Midstream

The midstream analysis includes transmission of the gas from 7G operations near Grande Prairie to a hypothetical Prince Rupert site in coastal B.C. for liquefaction (see map in Figure 2-5). Additionally, final pre-processing of the gas, which occurs at the liquefaction plant inlet, is included in the midstream stage. This pre-processing includes removal of any residual CO_2, H_2S, Hg, H_2O, as well as condensation of some of the heavier HC gases as LPG. We modeled these processes outside of OPGEE due to higher fidelity of available data from 7G datasets.

Emissions associated with transmission can be broken down into operational and non-operational emissions. Operational emissions are associated with gas combustion for compression and fugitives from compressor stations and pipelines. Non-operational emissions are embodied emissions associated with steel use in pipelines and land use changes. The pipeline route in the base case is 1,100 km long and has a 70 m wide right-of-way on average (see above for land use). The pipeline design contains seven compressor stations, of which four more remote stations are natural gas powered and three stations are grid-electric powered (electrified compression is preferred where feasibly close to existing electric grid). We use B.C. grid consumption intensity and GREET EFs to calculate emissions from pipeline operational energy use [48, 44]. EFs from the literature are used to estimate fugitives from compressor stations and pipelines [51, 39]. Embodied emissions

rely on GREET EFs for steel CI (as used in OPGEE) [52]. Land use emissions are calculated using the methodology described in the upstream portion of this analysis.

Pre-treatment for liquefaction consists of additional acid gas removal, dehydration, removal of additional fractions of heavier HCs (known as a deep cut), and pre-cooling of the gas for liquefaction. Engineering calculations done by 7G provided expected fuel consumption for these processes. All scenarios assume that a natural gas turbine powers these processes. Emissions from the gas turbines are calculated using GREET EFs.

Our land use emissions estimated using above methods align closely with those calculated for a proposed TransCanada pipeline following a roughly similar route. Scaling for differences in pipeline length, our value for land use impacts matches up exactly (99.7%) with that of the TransCanada estimate [45].

All parameters and assumptions used for calculations in the midstream stage of this analysis are listed in Table 2-12.

Table 2-12. Parameters and assumptions used in the midstream stage of this analysis.

Parameter Description	Value	Unit	Source	Notes
Pipeine Lifetime	30	[yrs]		
Gas Turbine Efficiency	40%	[-]		
Compressor Efficiency	84%	[-]		
Compressor Operation Time	24	[hrs/d]		
BC Grid Consumption Intensity	21.2	[g CO_2e/kWh]	[48]	
Compressor Station Fugitive Emissions Rate	621.5	[Mg CH_4/station-yr]	[39]	
Pipline Fugitive Emissions Rate	3.4	[Mg CH_4/km-yr]	[51]	
Total Pipeline Length	1100	[km]		
Pipeline Diameter	30	[in]		
Pipeline Wall Thickness	0.5	[in]		
Low Alloy Steel Density	0.3	[lb/in^3]	[52]	
Number of Compressor Stations	7	[-]		
Compressor Station Spacing	157	[km]		
Compressor Station Power Requirements				
Alberta Station 1 (NG)	38343	[hp]	[50]	
B.C. Stations 1-6 (3 NG/3 Electric)	47769	[hp]	[50]	
Compressor Station Ancillary Loads	10%	[-]		
Pre-treatment Fuel Consumption	3.3	[mmscf/d/bcf]	[50]	1
Deep Cut Fuel Consumption	7.7	[mmscf/d/bcf]	[50]	1
LPG Extracted during Deep Cut	64.02	[mmscf/d/bcf]	[50]	1
Consumption Scale-Up	1.07	[-]		1
Pre-treatment CompressionPower Requirement	67000	[hp]	[50]	

[1] 7G computed fuel cosumption requirements and corresponding liquids extraction based on 1 bcf NG input. We scale this upwards as we input ~1.1 bcf NG in base case.

2.2.5 Liquefaction

The liquefaction stage includes all activities between clean/pre-treated natural gas entering the liquefaction train and LNG entering the cargo hold of the transport ship. There are four sources of emissions in liquefaction: refrigeration/compression, ancillary power generation, flaring, and leaks/vents. Refrigeration/compression refers directly to the processes that cool the gas down to -162 °C. Ancillary power generation supports other on-site processes, such as the additional pre-processing required to remove trace contaminants. Flaring is traditionally a safety mechanism, with a lit flare allowing for large amounts of gas to be flared if a system upset were to occur. Leaks/vents, like in the upstream and

midstream stages, can be intentional or unintentional point source emissions of gas from equipment.

A detailed literature review undertaken by the University of Calgary provided energy consumption requirements per tonne of LNG produced including both compression/refrigeration processes and ancillary power generation. Flaring and fugitive factors from the literature review are provided in CO_2e emissions per tonne LNG. The literature review included various studies of existing LNG plants, focusing on EIAs rather than the academic literature. EIAs for Sabine Pass, Australia Pacific, Pluto, Gladstone, Snohvit, Qatar Gas 1 & 2, Gorgon, LNG Canada, and Pacific NW LNG are examined for the literature review. Ultimately, average power requirements from Pluto, Snohvit, Gorgon, and LNG Canada are used (due to data availability). Flaring emissions intensity is the average of Sabine Pass, Australia Pacific, Pluto, Gorgon, LNG Canada, and Pacific NW LNG. Fugitive emissions intensity is the average of Sabine Pass, Australia Pacific, Pluto, Gladstone, Gorgon, and LNG Canada. Values for fugitives appear low, much less than 0.1% of gas flow, while flaring rates are closer to 0.1% of gas flow.

Traditional liquefaction plants have relied on aero-derivative simple-cycle natural gas combustion turbine (NGCT) for power and shaft work. These simple cycle NGCT achieve a maximum efficiency of 39%. Use of combined cycle (NGCC) plants in place of simple-cycle NGCT would allow for significant emissions reductions from the liquefaction stage.

A third option for the liquefaction stage would be electric drive wherever feasible, powered by grid electricity. In terms of emissions intensity and cost, B.C. provides an appealing region for electric-drive liquefaction due to the low cost of power in the province and the low CI of their grid (both a product of the hydroelectric-dominated grid). If a liquefaction plant were able to reliably access grid power at the necessary scale, liquefaction related emissions would be near zero. Liquefaction via electricity faces some economic challenges and political hurdles, and therefore is not selected as the base case method.

The base case liquefaction stage assumes NGCC for electricity and shaft work, while the high emissions case assumes NGCT and the low emissions case assumes grid power is accessed.

All parameters and assumptions used for calculations in the liquefaction stage of this analysis are listed in Table 2-13.

Table 2-13. Parameters and assumptions used in the liquefaction stage of this analysis.

Parameter Description	Value	Unit	Source	Notes
Flaring Efficiency	98%	[-]		
Compressor Efficiency	84%	[-]		
NGCC Turbine Efficiency	54%	[-]	[57]	
Simple Cycle Turbine Efficiency	39%	[-]	[21]	
Electric Motor Efficiency	95%	[-]		
BC Grid Consumption Intensity	21.2	[g CO_2e/kWh]	[48]	
Flaring Emissions Intensity	3.30E-03	[t CO_2e/t LNG]		1
Fugitive Emissions Intensity	1.64E-03	[t CO_2e/t LNG]		1
Ancillary Loads Power Requirement	17.7	[MW/mmtpa LNG]		1
Compression Power Requirement	29.1	[MW/mmtpa LNG]		1

[1] Reliant on EIAs for existing and planned liquefaction plants. These values from University of Calgary literature review.

2.2.6 Transport

The transport stage accounts for berthing in B.C., shipping LNG via ocean tanker, berthing in China, and re-gasification of LNG. Emissions from berthing at the LNG plant are derived from literature values that provide CO_2e emissions per metric ton of LNG. These values come from the same studies examined in the liquefaction literature review (see above). Shipping emissions are computed using a methodology first used by Abrahams et al. [16]. EFs from Abrahams et al. were modified to align with EFs used in the rest of our work. Our results for transport differ from those presented by Abrahams et al. due to differences in shipping distance (and thus the amount of required re-gasification for propulsion). Shipping emissions account for berthing in China.

We assume that boil-off gas (BOG) is consumed by the tanker to fuel the majority of its trip to Shenzhen, China. BOG occurs naturally as heat transfer from the ambient environment warms the LNG, resulting in relatively small amounts of evaporation (0.125%/d). In some LNG transport ships, this gas is reliquified by on-board equipment rather than consumed, and diesel or bunker fuel is used as the primary fuel type. Such methods maximize the amount of LNG delivered to the port and reduce costs due to the low cost of bunker fuel per unit of energy compared to LNG. However, this method results in significantly higher CAP and GHG emissions, so we do not consider it here.

We maximize use of LNG in the system by assuming that any additional power required for the trip to Shenzhen – in excess of that provided by BOG – is provided by on-demand re-gasification of LNG. We assume the empty tanker must return to its port of origin, and thus cannot rely on BOG for the return trip. The base case assumes diesel is used to power the return trip, whereas the high emissions case assumes bunker fuel is used to fuel the return trip. In reality, there is no guarantee that the tanker would make a full return trip to B.C. Depending on supply and demand for tankers, the LNG ship could sail to (for example) Australia for refilling with LNG. However, the simplest assumption is that all tankers simply travel repeatedly between B.C. and China.

Re-gasification is an under-studied segment of the LNG life-cycle. Values in the literature are not presented using detailed calculations. As such, we use an average of literature values for re-gasification energy consumption based on seawater heat exchangers [16, 20]. Future work in this area should focus on first-order modeling of re-gasification processes. Re-gasification also offers large potential for emissions savings, as cooling processes could utilize the cooling potential from LNG and avoid refrigeration energy use. Japan, a long-term importer of LNG, has utilized this cooling potential for cryogenic power generation, cold storage, and air liquefaction and separation [53]. This study does not account for any such cases as no existing LNG re-gasification plants in China make use of the cooling potential of LNG.

All parameters and assumptions used for calculations in the transport stage of this analysis are listed in Table 2-14.

Table 2-14. Parameters and assumptions used in the transport stage of this analysis.

Parameter Description	Value	Unit	Source	Notes
Gas Expansion Ratio	600	[Vol NG/Vol LNG]	[16]	
Tanker LNG Capacity	260000	[m^3]		
Tanker Speed	19.5	[knots]	[16]	
Boil-off Gas Rate	0.125%	[%/d]	[16]	
Steam Engine Efficiency	30%	[-]	[16]	
Diesel Engine Efficiency	50%	[-]	[16]	
Engine Power @ Max	40000	[hp]	[16]	
Ship Berthing - Canada	1.16E-02	[t CO_2e/t LNG]		1
Shipping Regasification Power Requirement	3%	[NG Required / NG Regasified]	[16]	
Time at port	3	[d]		
Shipping Distance	9850	[km]		
Regasification Emissions Intensity (NETL)	17.7	[g CO_2e/kWh]	[20]	2
Power Generation Efficiency (NETL)	46.4%	[-]	[20]	2
Regasification Emissions Intensity (Abrahams et al.)	8	[g CO_2e/kWh]	[16]	2
Power Generation Efficiency (Abrahams et al.)	46%	[-]	[16]	2

[1] Value from University of Calgary Literature Review of EIAs

[2] We use generation efficiency to back-calculate correct emissions intensity for our analysis.

2.2.7 Downstream

The downstream stage includes transmission of re-gasified LNG in China and end-use consumption of the gas for either power generation or district heating.

Transmission from the re-gasification facility to a proposed power plant in Shenzhen requires a 30 km pipeline and one compressor station. We assume the compressor station to be natural gas-powered, and account for associated fugitive emissions [54]. Table 2-15 lists the parameters and assumptions used in the transmission of gas within China.

Table 2-15. Parameters and assumptions used in the downstream transmission stage of this analysis.

Parameter Description	Value	Unit	Source	Notes
Pipeline Distance	30	[km]		
Energy Intensity of NG Pipeline Transmission	372	[kJ/ton-km]	[54]	
NG Transmission Fuel Split			[54]	
NG	0.99	[%]		1
Electricity	0.01	[%]		1
Efficiency of NG Turbine	40%	[-]		
Efficiency of Compressor	84%	[-]		
Pipeline Fugitive Emissions Rate	3.4	[Mg CH_4/km-yr]	[51]	

[1] We assume this pipeline uses one natural gas-fired compressor station.

2.2.7.1 Electricity Generation Efficiency for Modern NGCC Plants

Modern NGCCs have very high thermal efficiencies. Brochures for NGCCs suggest efficiencies in excess of 60% on an LHV basis. For example, the Mitsubishi Hitachi Power Systems (MHPS) M501JAC has reported net efficiency in combined cycle configuration of 64.0% LHV basis [55]. Similarly, the GE 7HA.02 in a 1x1 combined cycle configuration has a reported LHV efficiency of 63.3% [56].

However, real-world efficiencies are generally lower than vendor-reported values. Reported values are measured using constant operations at International Organization for Standardization (ISO) standard testing conditions of 101.3 kPa, 15 °C, and 60% relative humidity. These reported values therefore do not include real-world inefficiencies associated with start-up and cool-down, part-load efficiency degradation, and operations at non-standard temperature, pressure, and humidity. For example, the MHPS turbine noted above will consume ~4% more gas per unit power produced at a compressor inlet temperature of 35 °C [55].

In order to better understand the efficiency of power generation using modern gas NGCC systems, we do not use ISO efficiencies and instead use reported statistics from operating power plants in the U.S. We use the transparent and detailed data available from the U.S. Energy Information Administration to obtain information on all NGCC plants installed in

the U.S. in 2015 and 2016, as well as the most advanced plants in the database, which does not yet appear in yearly U.S. Energy Information Administration (U.S. EIA) statistics.

Using data from U.S. EIA Form 860 [28], we selected NGCC power plants with first month of operation between 1/2015 and 12/2016, and rated output > 100 MW [57]. We use a similar process to filter data from Form 932 for the year 2016.

Instead of monthly provisional data for more recent years, the 2016 yearly data are used. For each plant, we collect yearly consumption of gas in MMBTU (higher heating value, HHV) and yearly power generation in MWh. We remove any plants from the above list that are listed with prime mover code "GT", as this corresponds to a simple-cycle gas turbine. For cases with prime mover code "GS", these represent single-shafts NGCC, so the efficiency is directly computable from yearly total MMBTU of gas consumed and yearly total MWh of power generated. For plants with two prime movers codes "CA" and "CT", these represent the steam and expansion turbines in a two-shaft NGCC systems. We sum natural gas use in MMBTU and power generated in MWh for both prime movers. We then compare this to electricity generated for both prime movers. In most cases, fuel consumption in prime mover code "CA" is minimal, due to this corresponding to supplemental duct firing in the heat recovery steam generator (HRSG), which is often a smaller source of combustion.

The resulting efficiencies represent HHV (gross) operating efficiencies due to U.S. EIA reporting fuel use in HHV units. To convert to LHV basis efficiencies we assume a gas composition (molar basis) of 92% CH_4, 4% C_2H_6, 1% C_3H_8, and 3% inert CO_2 and N_2. The LHV/HHV ratio is therefore 0.9016, or 90.16% MJ LHV/MJ HHV.

The resulting plant efficiencies for these plants are reported in Table 2-16.

Table 2-16. Reported calendar year 2016 efficiencies for natural gas combined cycle plants in U.S. with month of first operation between 1/2015 and 12/2016. Data from U.S. EIA Form 860 and Form 923 [57].

Plant	Operator	Efficiency [MJ electricity / MJ gas input]	
		HHV basis	LHV basis
Port Everglades	Florida Power & Light Co	49.72%	55.14%
Scattergood	Los Angeles Department of Water & Power	47.24%	52.40%
Riverton	Empire District Electric Co	46.76%	51.87%
Brunswick County Power Station	Virginia Electric & Power Co	46.49%	51.56%
Panda Liberty Generation Plant	Panda Liberty O&M LLC	48.83%	54.16%
Panda Patriot Generation Plant	Panda Patriot O&M LLC	50.60%	56.12%
Carty Generating Station	Portland General Electric Co	48.61%	53.91%
Cherokee	Public Service Co of Colorado	47.49%	52.67%
Cane Run	Louisville Gas & Electric Co	50.68%	56.21%
Nelson Energy Center	Invenergy Services LLC	46.33%	51.38%
Garrison Energy Center LLC	Garrison Energy Center LLC	48.84%	54.17%
Woodbridge Energy Center	Woodbridge Energy Center	49.78%	55.21%
Panda Temple Power Station	PPG - O&M Panda Temple Power LLC	47.23%	52.39%
Newark Energy Center	Newark Energy Center, LLC	50.11%	55.57%
	Mean	***48.48%***	***53.77%***
	Median	***48.72%***	***54.04%***
	Standard deviation	***1.53%***	***1.70%***
	5-%ile	***46.43%***	***51.50%***
	25-%ile	***47.23%***	***52.39%***
	50-%ile	***48.72%***	***54.04%***
	75-%ile	***49.76%***	***55.19%***
	95-%ile	***50.63%***	***56.15%***

In addition to this large sample of recently-built plants, two of the very newest gas turbines installed in the U.S. are of ultra-high efficiency H and J-class combined cycle systems. The Colorado Bend II and Wolf Hollow power plants in Texas that were installed in mid-2017 each contain a set of two GE 7HA.02 turbines coupled with one HRSG each [58]. This 2x1 configuration is used when size economies induce investment in two expansion turbines to feed each HRSG. In addition, the Grand River Energy Center recently installed a MHPS M501J power plant [59], but data on that plant's operations are currently not available.

We can use these data to estimate LHV and HHV efficiencies for these newest turbines as presented in Table 2-17.

Table 2-17. Reported efficiencies for new H- and J-class turbines installed in the U.S. in 2017. Data from U.S. EIA Plant Level Electricity Browser [57].

	Colorado Bend II		**Wolf Hollow**	
Heating value basis	LHV	HHV	LHV	HHV
Number of observed months	8	8	8	8
Median	55.90%	50.40%	52.80%	47.60%
Mean	56.20%	50.70%	52.10%	47.00%
High	61.00%	55.00%	53.70%	48.40%
Low	53.00%	47.80%	48.30%	43.50%

We set downstream power plant efficiencies with this work in mind. The base case assumes a 54% efficient (LHV) NGCC plant, in line with the median efficiency observed from new power plants built in 2015 and 2016. The high-emissions case assumes a 48% efficient plant, meant to represent an older NGCC plant in operation. Lastly, the low-emissions case assumes a 60% efficient plant, representing an ultra-modern NGCC plant operating at near-ideal conditions. Colorado Bend II operated at a maximum efficiency of 61% in the first eight months of operation, indicating that consistently achieving 60% efficiency may be possible in the future.

In addition, we consider a case where the natural gas end-use is district heating rather than power generation. We assume LHV efficiency of district heating to be 85%. Our downstream analysis does not account for any fugitive emissions associated with distribution.

Chapter 3

3 Results

3.1 Leak Detection and Repair Survey Effectiveness

First, we present data on emissions profiles and the results of our persistence analysis. An important result is the prevalence of super-emitters in the emissions dataset. Super-emitters can be defined in multiple ways, but generally refer to a small number of emission points that contribute to a majority of emissions. For instance, Brandt et al. showed that the largest 5% of leaks typically contribute over 50% of total leakage volume [8]. As such, emissions reductions efforts should focus on detecting and fixing these super-emitters as fast as possible.

3.1.1 Emissions Profiles

We find that even within our sample size of 1,133 quantified leaks and vents from initial visits, a small number of emission sources emit far more than the median emissions rates. Furthermore, within individual component-types we find that outliers exist. For example, Figure 3-1 shows emissions rates from a subset of component types from our analysis, only examining super pad emissions sources. Most emissions amounts are centered around a low value, but outliers generally push the mean upwards from the median. For larger sample sizes, we see that the notion of "one emission factor fits all" is inherently flawed, with large variability between individual emissions sources. The near-zero emitters are largely unimportant to the overall picture, while outliers should be the target of emissions reductions. Many such figures could be created given the large number of leak categories and site types.

Table 3-1 shows the percentiles for each component type analyzed in the study, as well as counts of leaks and total emissions from each leak type (tanks excluded, due to lack of quantification data). The mean exceeds the median for nearly every component type, indicating the long-tailed nature of these distributions.

Table 3-1. Detailed emissions distribution information for all leak and vent types found during initial surveys of all 7G facilities. All emission measurement units in kg/hr.

Component Type	Count	Total Emissions [kg/hr]	Mean	5%	25%	Median (50%)	75%	95%
Actuator	26	7.45	0.29	0.01	0.01	0.05	0.20	1.54
Analyzer	14	1.34	0.10	0.01	0.04	0.09	0.13	0.22
Catadyne Heater	248	19.50	0.08	0.01	0.05	0.05	0.14	0.19
Chemical Injection Pump	54	8.39	0.16	0.01	0.01	0.02	0.06	0.37
Compressor, Cylinder Head	12	1.30	0.11	0.01	0.01	0.06	0.20	0.29
Controller	143	22.21	0.16	0.01	0.03	0.07	0.18	0.38
Engine (Including Fuel/Start Gas)	28	0.88	0.03	0.01	0.01	0.02	0.05	0.08
Flange Connection	15	0.45	0.03	0.01	0.01	0.01	0.03	0.09
Meter / Instrumentation	20	2.11	0.11	0.01	0.02	0.03	0.17	0.37
Misc	19	0.72	0.04	0.01	0.01	0.02	0.06	0.10
Open Ended Line / Vent	115	51.96	0.45	0.01	0.03	0.15	0.38	2.08
Other Tank	1	0.02	0.02	0.02	0.02	0.02	0.02	0.02
Pneumatic Pump	4	0.16	0.04	0.01	0.01	0.04	0.07	0.07
Pressure Safety Valve (PSV)	3	0.83	0.28	0.19	0.21	0.23	0.32	0.39
Pump Packing	4	0.32	0.08	0.01	0.02	0.04	0.10	0.20
Regulator	34	1.66	0.05	0.01	0.01	0.03	0.05	0.16
Threaded Connection	313	13.67	0.04	0.01	0.01	0.01	0.04	0.15
Valve	80	5.20	0.06	0.01	0.01	0.02	0.05	0.23

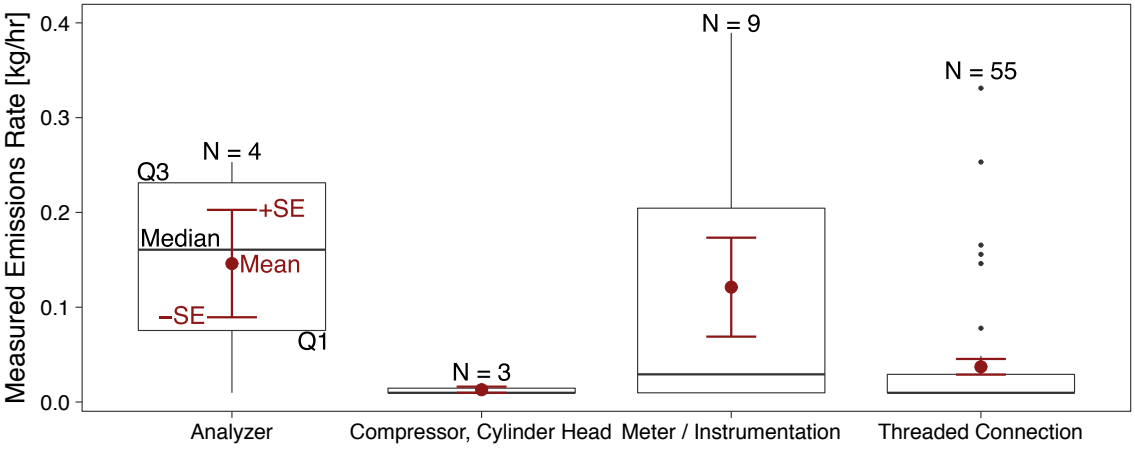

Figure 3-1. Emissions distribution for certain leak and vent types found during initial surveys at 7G super pads.

We also can plot a simple total distribution of all leaks and vents found and quantified at 7G sites, with site revisits excluded. Figure 3-2 shows the heavy-tailed distribution of leaks and vents. All data included in this figure come directly from measurements, without any supplemental data to account for detected leaks that were not quantified. As such, the expected largest emitting sources, tanks, are not included. Regardless, we find that the top 5% of emitters account for 51.6% of quantified emissions.

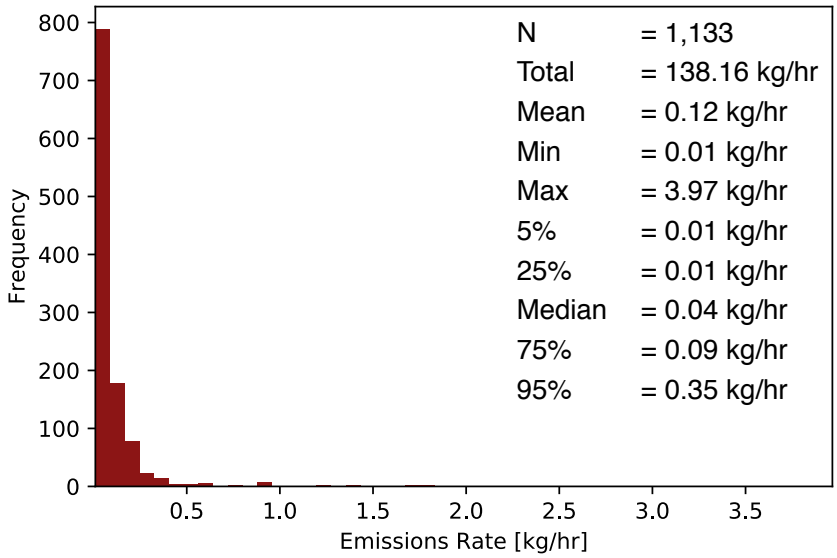

Figure 3-2. Distribution of quantified leak and vent emissions from initial visit 7G LDAR surveys.

3.1.2 Persistence Analysis

Four sites operated by 7G were visited two or more times in the datasets we had available. For three of these sites, we present results both in terms of number of detected emissions points and mass emissions rates. For these sites, we can classify leaks and vents as new or old sources. New sources are those not found in previous surveys, and old sources refer to a pre-existing emissions point that may or may not have been fixed before the resurvey. For one processing plant we show data from three surveys, but do not have the level of granularity to distinguish between new and old sources. Because 7G's operations are growing, many existing sites underwent equipment changes and expansions between surveys. Any major site changes or expansions are listed in Table 3-2. Results are presented in Figure 3-3 through Figure 3-6.

Table 3-2. Major site changes between initial and revisit surveys.

Site Name	Site Changes / Expansions
Satellite Pad 1	Four new wells brought online, including four new separator modules and necessary piperack extensions.
Satellite Pad 2	No major changes.
Compressor Station	No major changes.
Processing Plant	Increased condensate tank size from 750 bbl to 1000 bbl (between 2nd and 3rd visit).

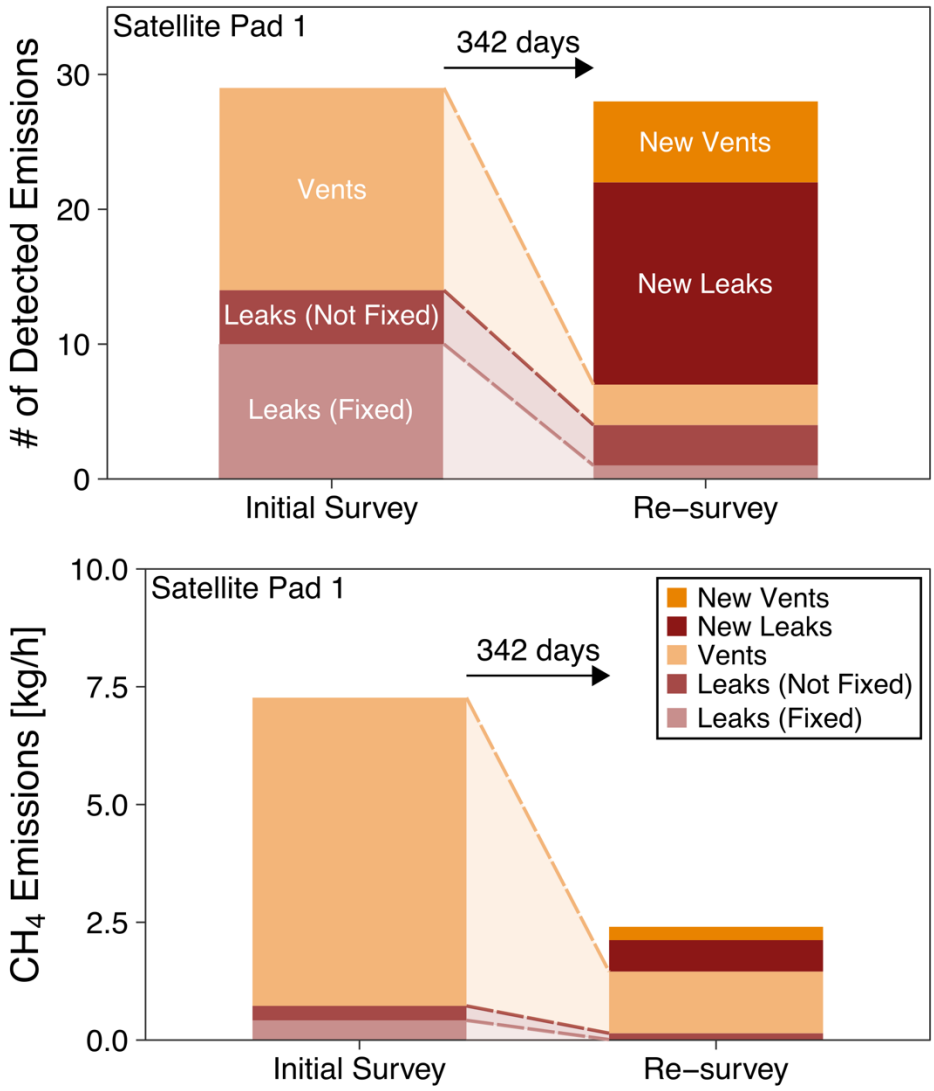

Figure 3-3. Persistence of leaks and vents for 7G satellite pad 1, in terms of number of detected emission points (top) and methane emissions rate (bottom).

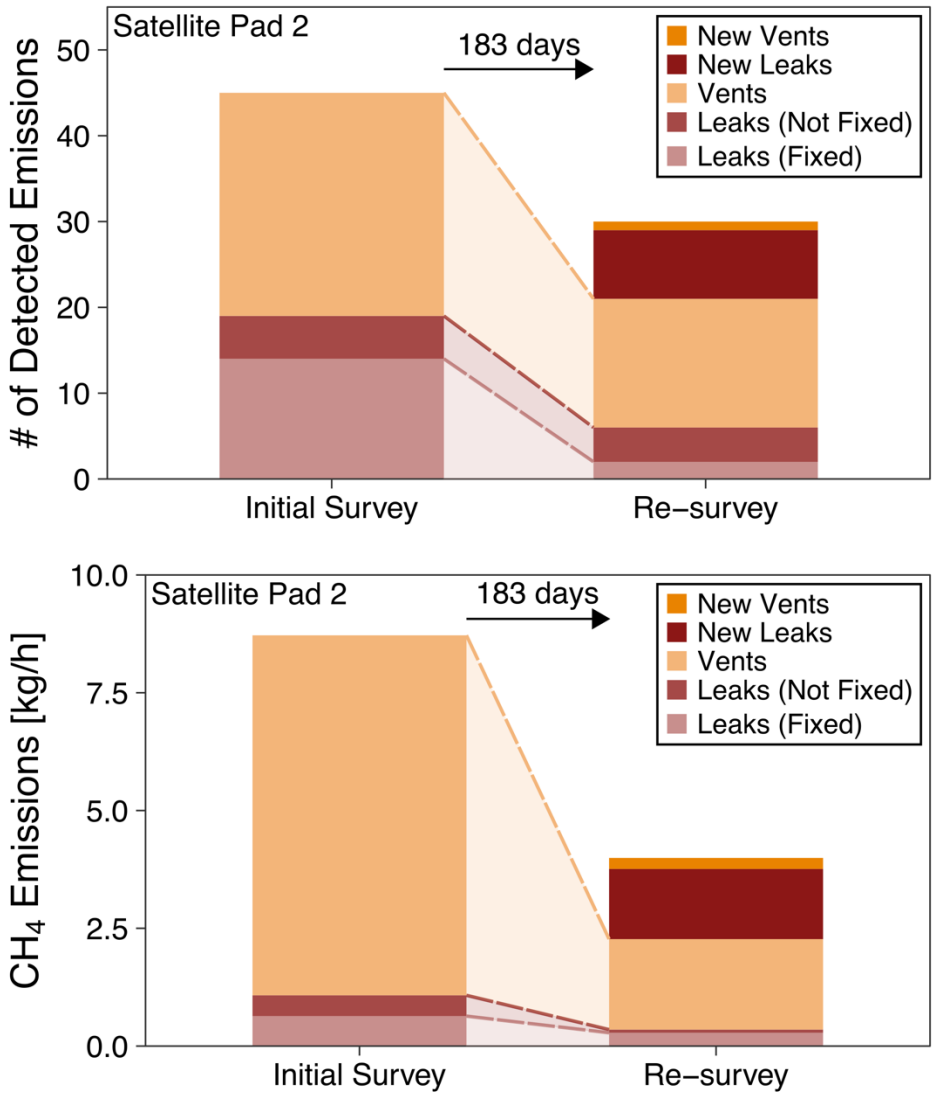

Figure 3-4. Persistence of leaks and vents for 7G satellite pad 2, in terms of number of detected emission points (top) and methane emissions rate (bottom).

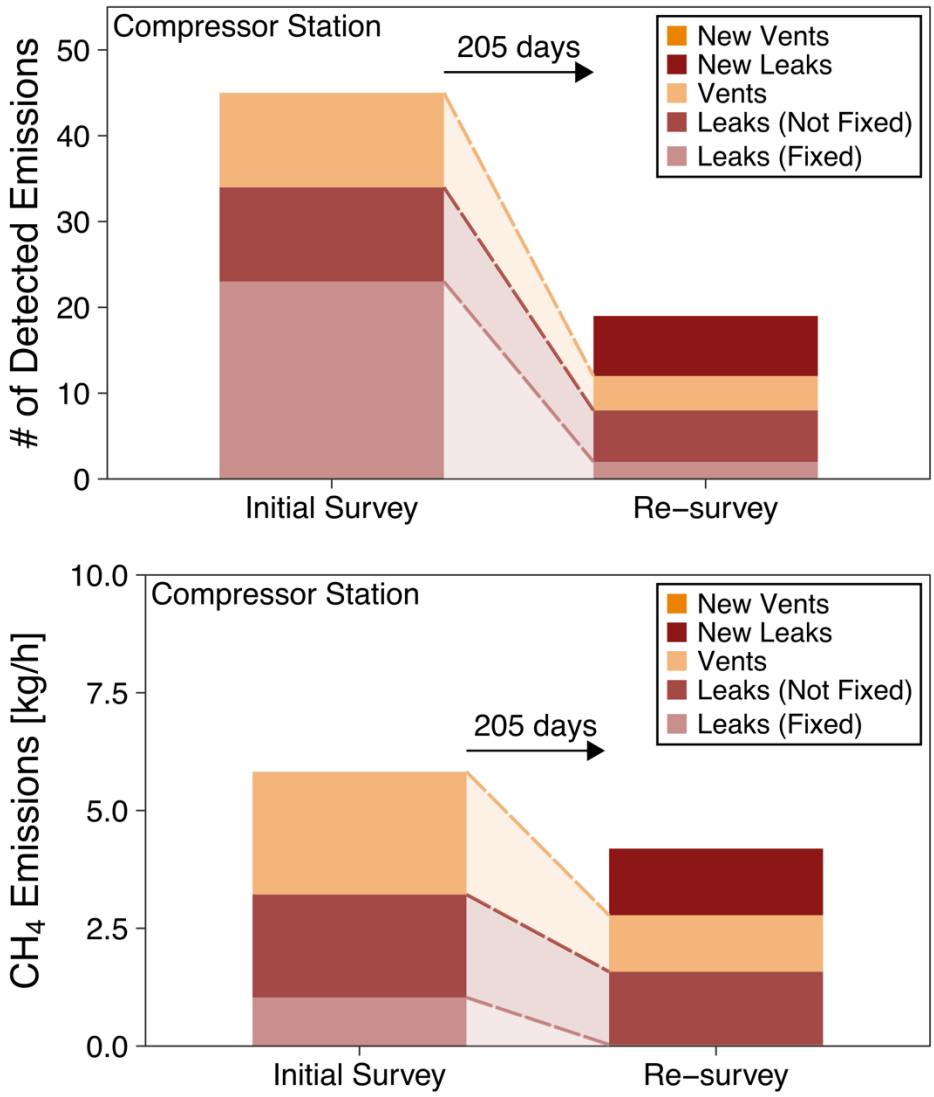

Figure 3-5. Persistence of leaks and vents for 7G compressor station, in terms of number of detected emission points (top) and methane emissions rate (bottom).

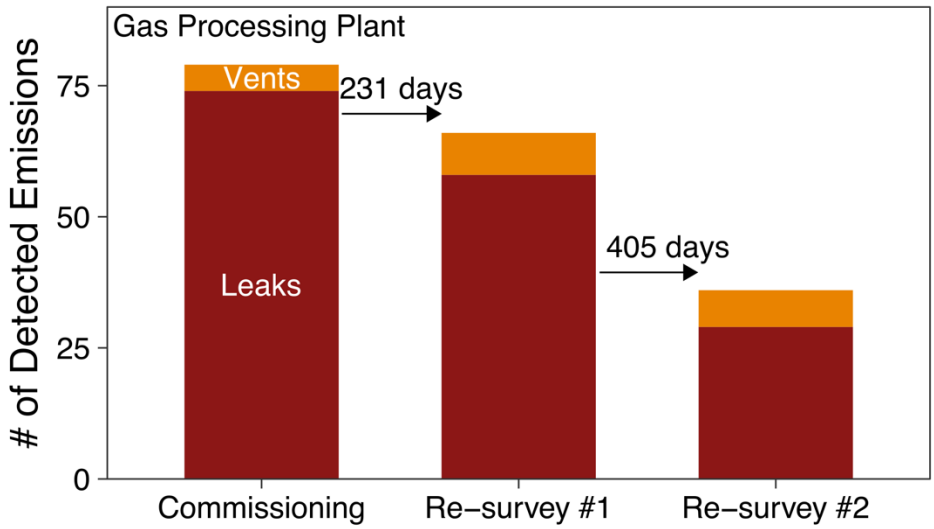

Figure 3-6. Persistence of leaks and vents for a gas processing plant over three surveys.

We find that in all cases, both the number of emissions points and the site-wide emissions rate decreased between repeat surveys. We also observed that leaks that were fixed tended to remain fixed and did not reappear. Likewise, leaks that were not fixed tended to persist and did not go away on their own, indicating that leak persistence is very high. Consequently, LDAR surveys are resulting in emissions reductions, so long as detected leaks are fixed. Repeat LDAR surveys regularly found new emission sources, even without significant site changes occurring, supporting the idea that LDAR surveys must be done regularly to find and fix new emission sources. Because emissions sources can arise from equipment failure or breakdown, repeated surveys are useful even in well-managed sites.

The decrease in vents found in repeat surveys was not solely due to intermittent venting or site changes. Catadyne heaters are seasonal pieces of equipment that are used to maintain a certain temperature near temperature-sensitive equipment. They are only utilized during cold weather events and are known for emitting large amounts of gas through poor combustion. 7G classifies these emission points as vents. In our datasets, initial visits tended to coincide with cold weather events, with many catadyne heaters operating. Revisits did not occur during such cold weather events, and as such, the number of catadyne heaters in use were far less. Thus, the large decrease in vents is not without explanation.

We also find that LDAR surveys performed at site commissioning are valuable, as equipment is either not properly installed, not fully tightened, or becomes strained under

initial production. Performing a survey at commissioning allows for these initial issues to be identified and fixed.

Overall, we conclude that emissions frequency and rate decreased with repeat LDAR surveys.

3.2 Life-cycle Assessment of Liquefied Natural Gas

We present results for both power generation and district heating end uses, though our discussion focuses on power generation results. Power generation life-cycle GHG emissions range from 408.6 to 548.4 g CO_2e/kWh. District heating emissions range from 80.32 to 86.2 g CO_2e/MJ heat. The larger range in power generation emissions is due to the range of power plant efficiencies analyzed in our cases. Results for selected GHG scenarios are summarized in Figure 3-7. Low, base, and high scenarios are described in Table 3-3.

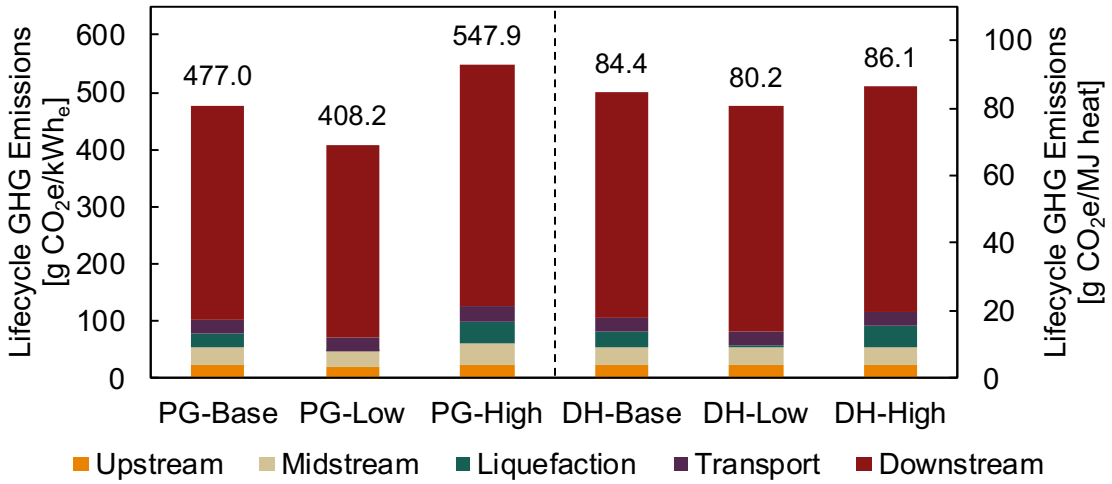

Figure 3-7. Life-cycle emissions by stage for various Power Generation (PG) and District Heating (DH) scenarios.

Table 3-3. Description of main scenarios for both power generation and district heating end-uses.

Scenario	Description
Base	Diesel fuel for shipping return trip, NGCC for liquefaction, power generation via NGCC operating at 54% LHV efficiency OR district heating at 85% efficiency.
Low	Diesel fuel for shipping return trip, B.C. Hydro for liquefaction, power generation via NGCC operating at 60% LHV efficiency OR district heating at 85% efficiency.
High	Bunker fuel for shipping return trip, simple-cycle NGCT for liquefaction, power generation via NGCC operating at 48% LHV efficiency OR district heating at 85% efficiency.

In addition to life-cycle GHG emissions, we also estimate life-cycle CAP emissions. We report emissions of NO_x, SO_x, PM_{10}, $PM_{2.5}$, black carbon (BC), and organic carbon (OC), normalized by electricity generated in our base case, in Figure 3-8.

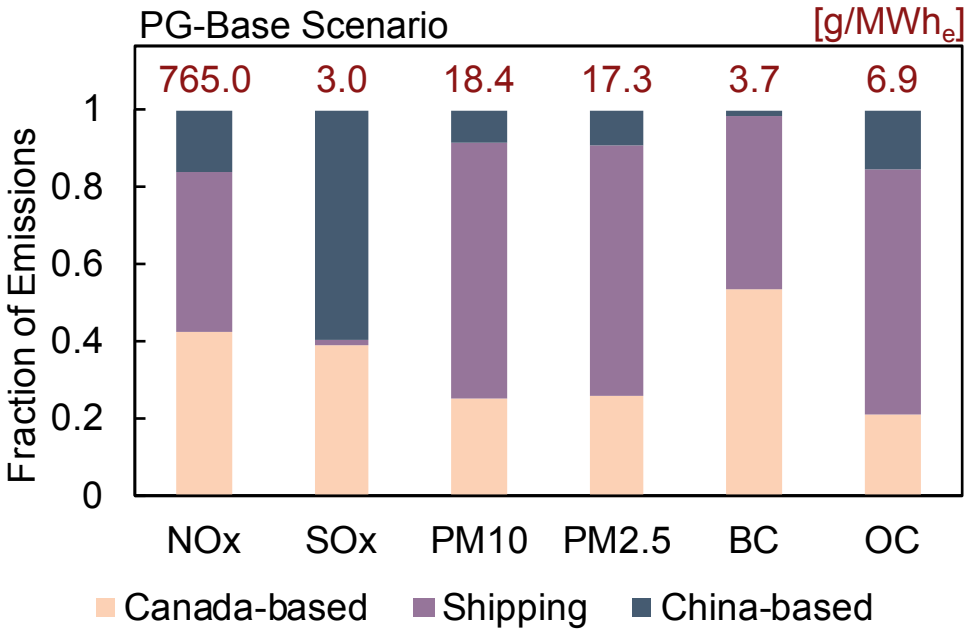

Figure 3-8. Normalized air pollutant emissions from our PG-base scenario.

Air pollutant emissions impacting local air quality occur primarily in Canada and over international waters (shipping). China will benefit tremendously if natural gas replaces coal generation, with natural gas burning much cleaner than coal. For example, coal air pollutant emissions in China have been estimated at 1,186 g NO_x/MWh, 713 g SO_x/MWh, and total particulate matter of 292 g/MWh, all far higher than their natural gas equivalents [60]. Canada, on the other hand, will have increased negative local air quality impacts. LNG production-for-export would be a new emissions source, not displacing any current power generation in Canada. Air pollutant emissions will increase in our PG-Low scenario due to bunker fuel consumption for shipping return trip. Figure 3-9 compares life-cycle emissions of NO_x and SO_x from our base case with Chinese coal.

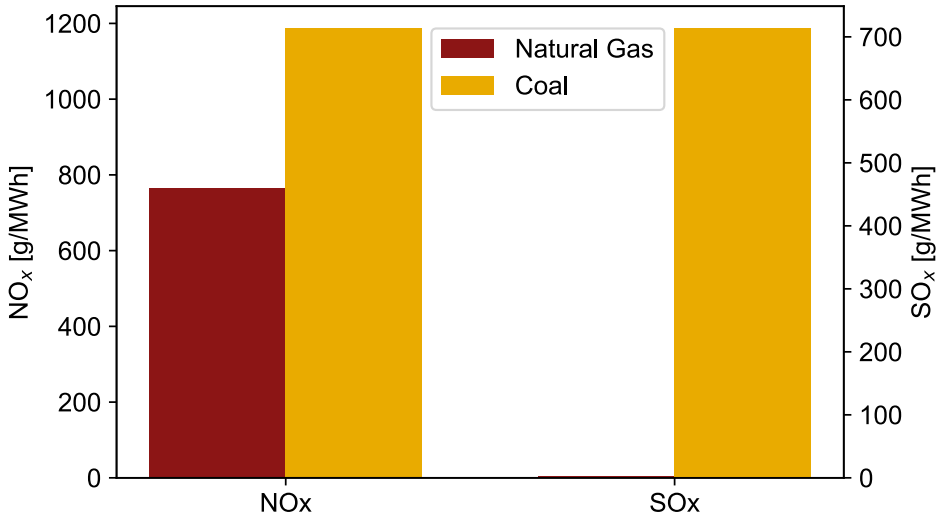

Figure 3-9. Life-cycle emissions of NO_x and SO_x for our base case and Chinese coal.

Life-cycle emissions in the PG case are dominated by end-use power generation. The PG-High case projects lower emissions than any projected by 15 comparison studies of the CI of LNG highlighted in Kasumu et al. [17]. Comparison with the results of Kasumu et al., as well as a study of coal life-cycle emissions by Yin et al., are presented in Figure 3-10.

Examining our results on PG life-cycle emissions intensity in more detail, we can understand the reasons for our lower emissions. Midstream and downstream emission estimates from the literature align well with our results, while upstream, liquefaction, and transport intensities from this study are generally lower than in the comparison studies. On average, 45% of the difference in life-cycle emissions can be explained by differences in upstream emissions, 30% by liquefaction, and 19% by transport.

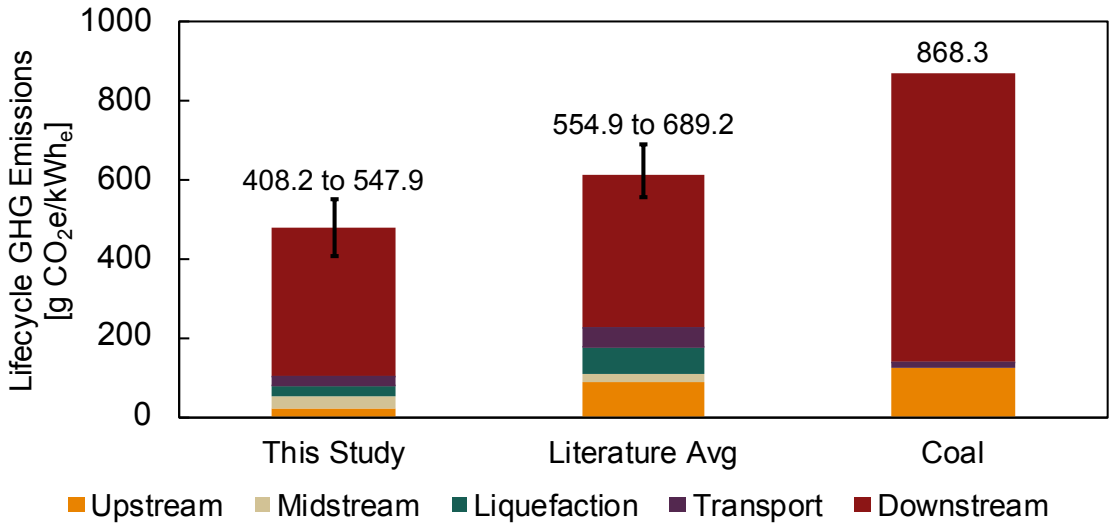

Figure 3-10. Life-cycle emissions by stage for our study, 15 comparison studies aggregated by Kasumu et al. [17]*, and average coal from Yin et al.* [60]*. Bar ranges represent low and high cases for our study, and range of results for comparison studies.*

The following sections present more-specific results for each stage and discuss some of the differences seen in the comparisons presented in Figure 3-10.

3.2.1 Upstream

Considerable effort was devoted to understanding the upstream emissions profile of 7G operations. Upstream emissions intensities, in terms of g CO_2e per MJ leaving the upstream stage, are presented in Table 3-4. Surface processing and fugitives dominate overall intensity. Surface processing refers primarily to combustion-related emissions associated with the treatment and separation of the production streams. Fugitives are leaks and operational vents that occur as part of the upstream production process. "Small sources" is a term in OPGEE accounting for remaining emissions sources that OPGEE does not directly model. A full list of emission sources known to be not counted for in OPGEE is available in the model spreadsheet. Offsite emissions are emissions from the generation of electricity used on-site, and emissions from steel, cement and other materials production for site equipment and wells.

Table 3-4. Upstream emissions by specific source. MJ of denominator is assessed at the field boundary.

Upstream Stage	Emissions Intensity [g CO_2e/MJ]
Exploration	0.00
Drilling & Development	0.09
Production & Extraction	0.01
Surface Processing	0.48
Maintenance	0.15
Offsite Emissions	0.29
Small Sources	0.50
Fugitives	0.46
Land Use	0.06
Office Heating / Cooling	0.00
Maintenance Trucks	0.00
Water Handling	0.19
Total	***2.24***

7G upstream emissions are lower than industry average. This is due to a variety of factors. First, their operations rely on newer equipment. Newer equipment tends to have emissions controls in place and operate at higher efficiencies. Second, less wear-and-tear on the system increases the likelihood that equipment functions as intended. Third, 7G has placed considerable importance on minimizing their upstream emissions profiles, through site design and proactive actions to reduce emissions (LDAR surveys, equipment upgrades, etc.).

Also of note, OPGEE takes a bottom-up approach to modeling processes and determining emissions. This approach has regularly estimated lower emissions compared with top-down approaches [7]. Our bottom-up approach to estimating fugitive emissions does not take episodic or intermittent emitting sources into account if they were not emitting during the 7G LDAR surveys. These time-dependent events may explain some of the differences between methods. Additionally, as a high-GOR producing field, emissions from gas production are expected to be lower than a primarily liquids producing field in which gas is treated largely as a waste product or flared such as the Bakken formation.

We modeled upstream emissions in OPGEE for each year over the 36-year project lifetime. Due to year-on-year changes, the intensity output from OPGEE decreased over time. Figure 3-11 presents emissions intensities from OPGEE for each modeled year (starting in

2017 and ending in 2052). Note that OPGEE output includes only emissions from exploration, drilling & development, production & extraction, surface processing, maintenance, offsite emissions, and small sources.

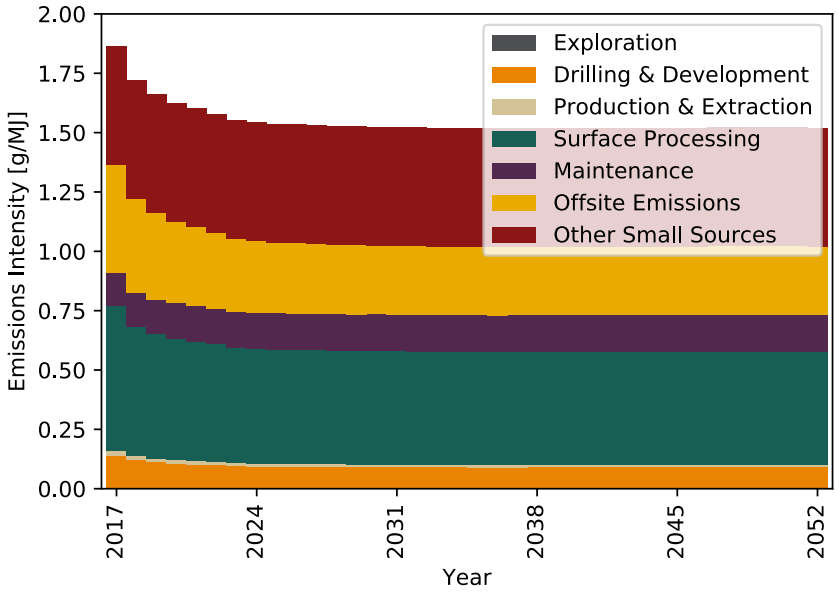

Figure 3-11. OPGEE emissions intensity output over time.

3.2.2 Midstream

Midstream emissions are larger than those from comparable studies. There are two possibilities for explaining this discrepancy. First, the proposed pipeline is around 1,100 km in length. The energy requirements for moving gas this distance is quite large, especially in comparison to gas projects that are located nearer to the coast (e.g. Pluto or Gorgon fields supplying large LNG projects in Australia). Second, the amount of pre-processing that is required depends on the composition and quality of the gas. Though the gas from 7G does not require significant processing, it is possible that some comparison fields require less processing (and thus have fewer associated emissions).

Table 3-5 presents emissions intensities in the base case for the midstream stage.

Table 3-5. Midstream emissions in the base case by specific source. MJ of denominator assessed at inlet terminus of LNG liquefaction train.

Midstream Stage	Emissions Intensity [g CO_2e/MJ]
Transmission - Operational	2.41
Transmission - Embodied	0.04
Transmission - Land Use	0.26
Pre-Treatment	1.47
Total	***4.17***

3.2.3 Liquefaction

Base case liquefaction emissions from this work are 0.17 t CO_2e/t LNG. These liquefaction emissions are lower than those in the academic literature but align well with those values reported in LNG EIAs. If we look at our high emissions case, which utilizes simple-cycle NGCT rather than NGCC for liquefaction, we estimate emissions of 0.24 t CO_2e/t LNG. A literature review of EIAs conducted by the University of Calgary indicates that emissions from simple-cycle NGCT-based liquefaction plants range from 0.22 to 0.35 t CO_2e/t LNG, with a mean of 0.29 ± 0.04 t CO_2e/t LNG. Thus, our case with NGCT power and liquefaction aligns with the lower end of the literature EIAs. Another comparison can be made to the LNG Canada EIA, which reports an expected emissions intensity of 0.12 t CO_2e/t LNG for a system where compression is done via simple-cycle NGCT, and ancillary power generation met with BC Hydro [21]. If we set our model to these assumptions, we estimate emissions of 0.16 t CO_2e/t LNG. Additional work is necessary to determine why modeled liquefaction emissions reported in academia are generally higher than those reported through EIAs.

Emissions intensities from the liquefaction stage are presented in Table 3-6 for different scenarios. The different scenarios refer to how power is provided for the compression and ancillary power processes. Emissions intensities for the grid power cases are significantly lower than the other cases due to the low CI of the B.C. grid. This analysis uses the average CI of the B.C. grid and does not account for marginal grid emissions.

Table 3-6. Liquefaction emissions by specific source. MJ of denominator assessed at outlet terminus of LNG liquefaction train.

Liquefaction Stage	Emissions Intensity [g CO_2e/MJ]			
	NGCC	Simple-cycle NGCT	B.C. Hydro for Ancillary Power	B.C. Hydro for Ancillary Power & Compression
Flaring & Fugitives	0.10	0.10	0.10	0.10
Compression & Ancillary Power	3.50	4.84	2.39	0.20
Total	***3.60***	***4.94***	***2.49***	***0.30***

We can compare these numbers with a collection of estimates on liquefaction stage emissions that were aggregated and presented in Abrahams et al. [16]. Table 3-7 provides these comparable emissions intensities.

Table 3-7. Liquefaction stage emissions from various studies. Reproduced from Abrahams et al. [16].

Source	Emissions Intensity [g CO_2e/MJ]
Hardisty 2012	8.06
Artecini 2010	6.51
Skone 2012	7.62
Skone 2014	8.24
Heede 2006	6.15
Verbeek 2011	5.90
LCFS	7.30
Cohen 2013	3.69
Biswas 2011	7.70
Yoon 1999	8.76
Okamura 2007	8.36
Tamura 2001	7.52
Yost 2003	3.83
Mean	***6.90***
Standard Deviation	***1.63***

Most studies likely assume a simple-cycle NGCT. Boundaries of these studies are unclear, but it is possible that pre-treatment emissions are included in some of these studies. If we include pre-treatment emissions with our simple-cycle NGCT case, we find an emissions intensity of 6.52 g CO_2e/MJ. This results in a number comparable with the mean from the listed studies. Some projects will need more intensive pre-treatment due to quality of the incoming gas stream, increasing emissions intensity. Nevertheless, these studies help show that while our liquefaction emissions intensity is comparable to formal EIAs of LNG

projects around the world, it is lower compared to the academic literature. Examining this difference requires further study.

3.2.4 Transport

Transport emissions can vary greatly based on LNG destination and tanker. Bunker fuel is considerably more emissions-intensive than a dual natural gas/diesel system that relies on BOG. Additionally, the re-gasification stage, which is grouped into this transport stage, is a relatively understudied area. As such, differences with comparison studies are not unexpected. Emissions intensities for the transport stage are presented in Table 3-8. Both presented cases use BOG for the initial trip, but use either diesel or bunker fuel for the return trip.

Table 3-8. Transport emissions by specific source. MJ of denominator assessed at outlet terminus of re-gasification facility.

Transport Stage	Emissions Intensity [g CO_2e/MJ]	
	Diesel	Bunker Fuel
Berthing - B.C.	0.25	0.25
Trans-Pacific Shipping	1.57	1.63
Regasification	1.68	1.68
Total	***3.50***	***3.56***

Re-gasification emissions are larger than shipping emissions, indicating that significant emissions savings exist if the cooling potential of LNG can be utilized in China. Future work is necessary to confirm the exact emissions intensity, and potential emissions savings, of re-gasification.

3.2.5 Downstream

The downstream stage dominates emissions from all other categories. Table 3-9 presents emissions intensities from the downstream stage, categorized by end-use and corresponding efficiency.

Table 3-9. Downstream emissions by specific source. MJ in denominator is MJ of electricity in the PG cases and MJ of useful heat in the DH case.

Downstream Stage	Emissions Intensity [g CO_2e/MJ]			
	PG: 48%	**PG: 54%**	**PG: 60%**	**DH: 85%**
Transmission	0.12	0.10	0.09	0.06
End-Use	117.44	104.39	93.95	66.53
Total	***117.55***	***104.49***	***94.04***	***66.59***

End-use emissions intensity varies greatly between cases. The low efficiency power generation case is 25% more emissions intensive than the high efficiency case. Clearly, small changes in power generation efficiency can quickly negate any benefits of upstream emissions reductions in LNG projects. The emissions intensity of district heating is much lower than that of power generation, as the conversion to heat is far more efficient. However, heat is a much lower quality energy resource (from an exergetic perspective).

3.2.6 Uncertainty

Except for the variant cases explored above, formal quantitative uncertainty analysis is not included in this study. In lieu of a quantitative uncertainty analysis, Table 3-10 discusses parts of the analysis and results that are inherently more uncertain.

Table 3-10. A qualitative survey of uncertainty in this study.

Stage	Uncertainty Level	Description
Upstream	Medium	Access to detailed data on 7G operations, site visits with real measurements, and significant time spent modeling upstream processes. Intermittent emission sources are not included, increasing the uncertainty level from low to medium.
Midstream	Low	Transmission energy requirements are well-understood, and sources of emissions fairly limited.
Liquefaction	High	Many unknowns here – and significant differences between what has been reported in EIAs and what has been modeled and reported in academia.
Transport	Medium	Tanker shipping emissions are well understood (low), but re-gasification remains under-studied and is not modeled in depth in this study (high).
Downstream	High	Power generation and district heating emissions are well-understood, but significant uncertainty remains in determining exact end-use of LNG in China.

Future LNG studies should consider the fact that end-use emissions dominate life-cycle emissions. Decreasing uncertainty in this stage is the best way to reduce overall uncertainty. Studies attempting to better understand how LNG will be used in China will be useful for determining the real-world GHG and air pollutant emissions impacts of Canadian-produced LNG. Additionally, re-gasification emissions are not insignificant, being similar in magnitude to shipping / transport emissions between B.C. and Shenzhen. Open-source models of the re-gasification process would contribute greatly to the academic literature. Finally, though upstream emissions in other studies are larger than we find here for 7G operations, these upstream emissions still pale in comparison to the total emissions from other stages. Upstream emissions nevertheless seem to attract the most attention. Time may be better spent modeling other processes in the LNG supply chain, if the goal is to best estimate life-cycle emissions.

Chapter 4

4 Discussion

Life-cycle analysis studies of LNG have tended to focus on the upstream and liquefaction stages. However, it is clear that total emissions are dominated by end-use. When considering the climate benefits and drawbacks of LNG, it is critical to understand where the gas will go and how it will be consumed.

The common assumption that LNG will displace coal on a one-to-one basis for power supply or district heat supply is not entirely clear. In fact, it is an actively researched area rife with scientific debate [61, 62]. With growing demand for energy in China, it is possible that the import of LNG would not replace any current generation and instead represent new generation that would otherwise not exist. Other possibilities to consider are that LNG would displace possible renewable generation, thereby undermining emissions reductions goals. Conversely, a system relying more heavily on natural gas is more flexible and should allow for higher penetration of intermittent renewables. We do not attempt to hypothesize which of these possibilities will occur, but note that environmental benefits of LNG pathways depend on displacing coal and not simply inducing additional consumption.

Those caveats noted, our work shows that Canada-to-China LNG will result in fewer life-cycle GHG emissions than the same power generated using coal in Asian markets. Studies have estimated such emissions to be anywhere from 868 to 975 g CO_2e/kWh, nearly double our results [60, 63].

Our work on LDAR programs, and the persistence of leaks and vents, has taken first steps towards quantifying the benefits of such programs. We have shown that LDAR programs are resulting in emissions reductions, and that emission points are likely to persist without any action taken. As our world becomes more dependent on gas, it will be important to minimize emissions associated with its production. LDAR surveys are proving to be a reliable means of reducing emissions from upstream sites.

As policy makers and stakeholders look at implementing these programs, they must consider the importance of the ability of the human surveyor. As we have shown, survey results can differ wildly depending on surveyor. For emissions reductions to be fully realized, surveyors must be competent. This is not to say that every emission point must be found – the vast majority of emission sources are negligible when looking at total emissions. However, we must ensure that the intent of an LDAR survey is not just to check a regulatory box, but rather to realize true emissions reductions.

As with any body of work, there are future steps to be taken and ways of improving on the work we have done. One key shortcoming of this work is its handling of re-gasification. Many studies rely on literature values, but our reliance on "black box" numbers with little insight as to how they were determined is a weakness of this work. Future efforts to model the physical processes of re-gasification would be immensely valuable. As we have shown that downstream emissions are much larger than any other stages in the LCA, additional work exploring how gas will be used is of vital importance. A more detailed analysis could consider specific turbines, selected from the Gas Turbine Engineering Handbook [64]. Turbine-specific EFs, impacts of degradation over time, and insights into real-world operating conditions would help us better assess downstream emissions.

Additionally, 7G has plans to continue performing regular LDAR surveys. As this data becomes available, it will be important to see how emissions reductions change over time. As this work relies on a small sample size of revisited sites, we can further back up our claims with a more robust dataset. Future studies should attempt to recreate our persistence analysis for other producers and different producing regions. 7G is a new producer, having begun production less than a decade ago. This means the majority of their sites are still relatively new, with equipment that has not had to suffer decades of wear-and-tear. The general scientific literature would benefit greatly from similar studies done with operators of older sites and smaller producers.

Nomenclature

Abbreviations

7G:	Seven Generations Energy Ltd.
B.C.:	British Columbia
BOG:	Boil-off Gas
CAP:	Criteria Air Pollutant
CI:	Carbon Intensity
Davis:	Davis Safety Ltd.
EF:	Emission Factor
EIA:	Environmental Impact Assessment
GHG:	Greenhouse Gas
GOR:	Gas-oil Ratio
GREET:	Greenhouse gases, Regulated emissions, and Energy use in Transportation
GWP:	Global Warming Potential
HC:	Hydrocarbon
HD:	Hyperbolic Decline
HHV:	Higher Heating Value
HRSG:	Heat Recovery Steam Generator
IR:	Infrared
ISO:	International Organization for Standardization
LCA:	Life-cycle Assessment
LDAR:	Leak Detection and Repair
LHV:	Lower Heating Value
LNG:	Liquefied Natural Gas
LPG:	Liquefied Petroleum Gas
MHPS:	Mitsubishi Hitachi Power Systems
NETL:	National Energy Technology Laboratory
NGCC:	Natural Gas Combined Cycle
NGCT:	Natural Gas Combustion Turbine
NGL:	Natural Gas Liquid
OGI:	Optical-gas Imaging
OPGEE:	Oil Production Greenhouse Gas Emissions Estimator
PLR:	Proportional Loss Rate
qOGI:	Quantitative Optical-gas Imaging
RMSE:	Root Mean Square Error
SE:	Stretched Exponential
U.S.:	United States
U.S. EIA:	U.S. Energy Information Administration
VOC:	Volatile Organic Compound

Units

bbl:	Barrel
bcf:	Billion cubic feet
CFM:	Cubic Feet per Minute
d:	Day
g:	Grams
Ha:	Hectare
hr:	Hour
kg:	Kilogram
kWh:	Kilowatt hour
L:	Liter
m^3:	Meters cubed
min:	Minute
MJ:	Megajoule
mmbtu:	Million British thermal units
mmscf:	Million standard cubic feet
MWh:	Megawatt hour
s:	Second
scf:	Standard cubic feet
t:	Metric ton, tonne
tcf:	Trillion cubic feet

Chemical Species

BC:	Black Carbon
C:	Carbon
CH_4:	Methane
C_2H_6:	Ethane
C_3H_8:	Propane
CO_2:	Carbon Dioxide
CO_2e:	Carbon Dioxide Equivalent
Hg:	Mercury
H_2O:	Water
H_2S:	Hydrogen Sulfide
N_2:	Nitrogen gas
NO_x:	Nitrogen Oxide
OC:	Organic Carbon
$PM_{2.5}$:	Particulate Matter (diameter less than 2.5 micrometers)
PM_{10}:	Particulate Matter (diameter less than 10 micrometers)
SO_x:	Sulfur Oxide

References

[1] U.S. Energy Information Administration, "Net Generation by Energy Source: Total (All Sectors), 2006 - 2016," 7 12 2017. [Online]. Available: https://www.eia.gov/electricity/annual/html/epa_03_01_a.html.

[2] J. Kearns, H. Dormido and A. McDonald, "China's War on Pollution Will Change the World," *Bloomberg,* 9 3 2018.

[3] U.S. Energy Information Administration, "U.S. Shale Gas Production," 13 2 2018. [Online]. Available: https://www.eia.gov/dnav/ng/hist/res_epg0_r5302_nus_bcfa.htm .

[4] U.S. Energy Information Administration, "Henry Hub Natural Gas Spot Price," 6 6 2018. [Online]. Available: https://www.eia.gov/dnav/ng/hist/res_epg0_r5302_nus_bcfa.htm .

[5] H. M. El-Houjeiri, M. S. Masnadi, K. Vafi, J. Duffy and A. R. Brandt, "Oil Production Greenhouse Gas Emissions Estimator: OPGEE v2.0 User guide & Technical documentation," 2017.

[6] Environmental Assessment & Optimization Group, [Online]. Available: https://eao.stanford.edu.

[7] A. Brandt, G. Heath, E. Kort, F.O'Sullivan, G. Pétron, S. M. Jordaan, P. Tans, J. Wilcox, A. M. Gopstein, D. Arent, S. Wofsy, N. Brown, R. Bradley, G. Stucky, D. Eardley and R. Harriss, "Methane Leaks from North American Natural Gas Systems," *Science,* vol. 343, no. 6172, pp. 733-735, 2014.

[8] A. R. Brandt, G. A. Heath and D. Cooley, "Methane Leaks from Natural Gas Systems Follow Extreme Distributions," *Environmental Science & Technology,* vol. 50, no. 22, pp. 12512-12520, 2016.

[9] R. A. Alvarez, S. W. Pacala, J. J. Winebrake, W. L. Chameides and S. P. Hamburg, "Greater focus needed on methane leakage from natural gas infrastructure," *Proceedings of the National Academy of Sciences of the United States of America,* vol. 109, no. 17, pp. 6435-6440, 2012.

[10] Environmental Defense Fund, "Methane Research: The 16 Study Series," 2018. [Online]. Available: https://www.edf.org/sites/default/files/methane_studies_fact_sheet.pdf.

[11] D. T. Allen, V. M. Torres, J. Thomas, D. W. Sullivan, M. Harrison, A. Hendler, S. C. Herndon, C. E. Kolb, M. P. Fraser, A. D. Hill, B. K. Lamb, J. Miskimins, R. F. Sawyer and J. H. Seinfeld, "Measurements of methane emissions at natural gas production sites in the United States," *Proceedings of the National Academy of Sciences of the United States of America,* vol. 110, no. 44, pp. 17768-17773, 2013.

[12] International Energy Agency, "World Energy Outlook," 2017. [Online]. Available: https://www.iea.org/newsroom/energysnapshots/marginal-abatement-cost-curve-for-oil-and-gas-methane-related-emissions.html.

[13] B. H. Powell, "Climate Change Legal Roadmap: Methane Reduction under the Climate Change Leadership Plan," Environmental Law Centre, Edmonton, 2017.

[14] Carbon Limits, "Statistical Analysis of Leak Detection And Repair Programs in Europe," Oslo, 2017.

[15] J. W. Coleman, A. Kasumu, J. Liendo, V. Li and S. M. Jordaan, "Calibrating Liquefied Natural Gas Export Life Cycle Assessment: Accounting for Legal Boundaries and Post-Export Markets," *Canadian Institute of Resources Law, Occasional Paper No. 49,* 2015.

[16] L. S. Abrahams, C. Samaras, W. M. Griffin and H. S. Matthews, "Life Cycle Greenhouse Gas Emissions From U.S. Liquefied Natural Gas Exports: Implications for End Uses," *Environmental Science & Technology,* vol. 49, no. 5, pp. 3237-3245, 2015.

[17] A. S. Kasumu, V. Li, J. W. Coleman, J. Liendo and S. M. Jordaan, "Country-level Life Cycle Assessment of Greenhouse Gas Emissions from Liquefied Natural Gas Trade for Electricity Generation," *Environmental Science & Technology,* vol. 52, no. 4, pp. 1735-1746, 2018.

[18] S. Yeh, A. Ghandi, B. R. Scanlon, A. R. Brandt, H. Cai, M. Q. Wang, K. Vafi and R. C. Reedy, "Energy Intensity and Greenhouse Gas Emissions from Oil Production in the Eagle Ford Shale," *Energy Fuels,* vol. 31, no. 2, pp. 1440-1449, 2017.

[19] A. R. Brandt, T. Yeskoo, M. S. McNally, K. Vafi, S. Yeh, H. Cai and M. Q. Wang, "Energy Intensity and Greenhouse Gas Emissions from Tight Oil Production in the Bakken Formation," *Energy Fuels,* vol. 30, no. 11, pp. 9613-9621, 2016.

[20] National Energy Technology Laboratory, "Life Cycle Greenhouse Gas Perspective on Exporting Liquefied Natural Gas from the United States.," 2014.

[21] The Delphi Group, " LNG Production in British Columbia: Greenhouse Gas Emissions Assessment and Benchmarking," BC Climate Action Secretariat, Ontario, 2013.

[22] AECOM, "Prince Rupert LNG," Burnaby, 2013.

[23] Environmental Assessment Office, "Kitimat LNG Terminal Environmental Assessment Certificate Application," 2006.

[24] Environmental Assessment Office, "Pacific Northwest LNG Project Assessment Report," 2014.

[25] C. E. Kemp, A. P. Ravikumar and A. R. Brandt, "Comparing Natural Gas Leakage Detection Technologies Using an Open-Source “Virtual Gas Field” Simulator," *Environmental Science & Technology,* vol. 50, no. 8, pp. 4546-4553, 2016.

[26] A. P. Ravikumar, J. Wang and A. R. Brandt, "Are Optical Gas Imaging Technologies Effective For Methane Leak Detection?," *Environmental Science & Technology,* vol. 51, no. 1, pp. 718-724, 2017.

[27] T. Howard, T. W. Ferrara and A. Townsend-Small, "Sensor transition failure in the high flow sampler: Implications for methane emission inventories of natural gas

infrastructure," *Journal of the Air & Waste Management Association,* vol. 65, no. 7, pp. 856-862, 2015.

[28] R. A. Alvarez, D. R. Lyon, A. J. Marchese, A. L. Robinson and S. P. Hamburg, "Possible malfunction in widely used methane sampler deserves attention but poses limited implications for supply chain emission estimates," *Elementa Science of the Anthropocene,* vol. 4, no. 137, 2016.

[29] Providence Photonics, "Quantitative Optical Gas Imaging," 2018. [Online]. Available: https://www.providencephotonics.com/leak-quantification.

[30] Rebellion Photonics, "Products," 2018. [Online]. Available: https://rebellionphotonics.com/products.html.

[31] FLIR Systems, Inc., "Industrial Gas Detection Cameras," 2018. [Online]. Available: https://www.flir.com/.

[32] J. Englander, *METEC Site Photos,* Fort Collins, 2018.

[33] Heath Consultants Incorporated, "Hi Flow Sampler," 2018. [Online]. Available: http://heathus.com/wp-content/uploads/hiflow.pdf.

[34] National Gas Machinery Laboratory, "Cost-Effective Directed Inspection and Maintenance Control Opportunities at Five Gas Processing Plants and Upstream Gathering Compressor Stations and Well Sites," Manhattan, 2006.

[35] R. Subramanian, L. L. Williams, T. L. Vaughn, D. Zimmerle, J. R. Rosciolio, S. C. Herndon, T. I. Yacovitch, C. Floerchinger, D. S. Tkacik, A. L. Mitchell, M. R. Sullivan, T. R. Dallmann and A. L. Robinson, "Methane Emissions from Natural Gas Compressor Stations in the Transmission and Storage Sector: Measurements and Comparisons with the EPA Greenhouse Gas Reporting Program Protocol," *Environmental Science & Technology,* vol. 49, no. 5, pp. 3252-3261, 2015.

[36] E. D. Thoma, P. Deshmukh, R. Logan, M. Stovern, C. Dresser and H. L. Brantley, "Assessment of Uinta Basin Oil and Natural Gas Well Pad Pneumatic Controller Emissions," *Journal of Environmental Protection,* vol. 8, no. 4, pp. 394-415, 2017.

[37] J. Kuo, "Estimation of Methane Emissions From the California Natural Gas System," California Energy Commission, 2012.

[38] D. R. Lyon, R. A. Alvarez, D. Zavala-Araiza, A. R. Brandt, R. B. Jackson and S. P. Hamburg, "Aerial Surveys of Elevated Hydrocarbon Emissions from Oil and Gas Production Sites," *Environmental Science & Technology,* vol. 50, no. 9, pp. 4877-4886, 2016.

[39] D. J. Zimmerle, L. L. Williams, T. L. Vaughn, C. Quinn, R. Subramanian, G. P. Duggan, B. Willson, J. D. Opsomer, A. J. Marchese, D. M. Martinez and A. L. Robinson, "Methane Emissions from the Natural Gas Transmission and Storage System in the United States," *Environmental Science & Technology,* vol. 49, no. 15, pp. 9374-9383, 2015.

[40] Eastern Research Group, Inc., "City of Fort Worth Natural Gas Air Quality Study," Morrisville, 2011.

[41] Intergovernmental Panel on Climate Change, *Fourth Assessment Report,* 2007.

[42] S. McNally, "A characterization of productivity, recovery, and future oil production potential of the Bakken formation of North Dakota," 2014.

[43] M. Masnadi, *EAO Research Group Internal Presentation on OPGEE,* Stanford, CA, 2017.

[44] Argonne National Laboratory, "The Greenhouse gases, Regulated Emissions, and Energy use in Transportation Model," 2017.

[45] TransCanada, "Coastal GasLink Pipeline Project: Greenhouse Gas Emissions Technical Data Report," 2014.

[46] S. Yeh, A. Zhao, S. D. Hogan, A. R. Brandt, J. G. Englander, D. W. Beilman and M. Q. Wang, "Past and Future Land Use Impacts of Canadian Oil Sands and Greenhouse Gas Emissions," UC Davis Institute of Transportation Studies, 2015.

[47] Canada's National Forest Inventory, "Revised 2006 baseline, version 3," 2013.

[48] Environment and Climate Change Canada, "National Inventory Report 1990-2015: Greenhouse Gas Sources and Sinks in Canada," Quebec, 2017.

[49] Seven Generations Energy Ltd., "CDP Oil and Gas Sector Module 2017 Drafting Document," 2017.

[50] Seven Generations Energy Ltd., "Internal Document for Life-cycle Assessment Work," 2017.

[51] D. Picard, "Fugitive Emissions from Oil and Natural Gas Activities," in *Good Practice Guidance and Uncertainty Management in National Greenhouse Gas Inventories*, 1999.

[52] R. Mitchell, "Casing Design," in *Drilling Engineering*, USA: Society of Petroleum Engineers, 2006.

[53] M. Corkhill, "Cold energy extracts value from the LNG supply chain," *LNG World Shipping,* 13 October 2016.

[54] X. Ou, Y. Xiaoyu and X. Zhang, "Life-cycle energy consumption and greenhouse gas emissions for electricity generation and supply in China," *Applied Energy,* vol. 88, no. 1, pp. 289-297, 2011.

[55] Mitsubishi Hitachi Power Systems, "Gas Turbine Combined Cycle (GTCC) Power Plants," 2018. [Online]. Available: https://www.mhps.com/products/gtcc/index.html.

[56] General Electric, "GE's HA Gas Turbine Fleet," 2018. [Online]. Available: https://www.gepower.com/gas/gas-turbines/h-class.

[57] U.S. Energy Information Administration, "Electricity Data Browser," 2018. [Online]. Available: https://www.eia.gov/electricity/data/browser/.

[58] P. Olson, "Small Change, Big Effect: GE Gas Turbines Improve Power Plant Efficiency in Texas," 21 February 2017. [Online]. Available: https://www.gepower.com/about/insights/articles/2017/02/powering-texas-exelon.

[59] Editors of Power Engineering, "First J-Series Gas Turbine in Americas Now Operational," *Power Engineering,* 31 5 2017.

[60] L. Yin, Y. Liao, L. Zhou, Z. Wang and X. Ma, "Life cycle assessment of coal-fired power plants and sensitivity analysis of CO2 emissions from power generation side," *IOP Conference Series: Materials Science and Engineering,* vol. 199, 2017.

[61] A. Q. Gilbert and B. K. Sovacool, "US liquefied natural gas (LNG) exports: Boom or bust for the global climate?," *Energy,* vol. 141, pp. 1671-1680, 2017.

[62] M. A. MacKinnon, J. Brouwer and S. Samuelsen, "The role of natural gas and its infrastructure in mitigating greenhouse gas emissions, improving regional air quality, and renewable resource integration," *Progress in Energy and Combustion Science,* vol. 64, pp. 62-92, 2018.

[63] H. Hondo, "Life cycle GHG emission analysis of power generation systems: Japanese case," *Energy,* vol. 30, 2005.

[64] M. P. Boyce, Gas Turbine Engineering Handbook, Elsevier Science, 2011.